NULL DYNAMICS OF CLASSICAL MAXWELL–DIRAC FIELDS

J.G. CARDOSO*

Department of Mathematics, Quaid-i-Azam University
Islamabad, Pakistan

(Received March 10, 1994)

Null initial data techniques are used to describe the dynamics of classical Maxwell–Dirac fields in real Minkowski space. On the basis of the structure of the field equations a graphical device is constructed which enables one to unambiguously label elements of the corresponding infinite invariant exact set in terms of colored trees. The complete specification of the trees arises naturally from the procedures involved in the actual evaluation of the elementary contributions. Each tree turns out to be associated with a manifestly finite scaling invariant integral which is taken over a compact space of appropriate null configurations. In particular the integrals describing the processes of electromagnetic scattering of Dirac fields appear to be taken over spaces of forked null zigzags that start at the origin and terminate at a fixed point lying in the interior of the future cone of the origin.

PACS numbers: 03.65. Pm

1. Introduction

Null initial data (NID) techniques [1–3] constitute a general framework for describing the dynamics of sets of interacting spinor fields in both flat and curved space-times. This null approach was designed to treat a form of initial value problem in which the initial data for all fields are specified at non-singular points of null hypersurfaces. Loosely speaking, the elements of an NID set for some system are defined as those field components which are associated with the directions of generators of a null hypersurface. In general, each such initial datum carries twice as much information per space-time point as does each of the data involved in the corresponding space-like

* Present address: Department of Mathematics, Centre for Technological Sciences–UDESC, Joinville 89223–100, Santa Catarina, Brazil.

hypersurface initial value problem, insofar as an arbitrary null datum is locally specified by a pair of real numbers. Hence, a set of null hypersurface initial data generally provides one-half the number of real-valued scalar functions that is required in the ordinary space-like approach. One of the key concepts upon which these techniques are based is that of an invariant exact set (IES). The striking feature of such a field set is that the (local) algebraic relations defining its exactness do not involve gauge-dependent quantities explicitly. All interactions thus appear to be controlled by the field equations or else by Lorentz-invariant commutation relations which involve covariant derivatives of the fields along with the fields themselves. Once we are given an IES, we can state that the field equations propagate the fields in a non-redundant way throughout the relevant space-time domain. Likewise, all the constraints which would occur in the space-like treatment are at the outset automatically eliminated from the basis of the theories.

According to the conventional methods, the evaluation of the fields is carried out by using either power series expansions or integral devices. In the former case, one usually requires the fields to be analytic on their domain of definition. In the event that the fields constitute an IES, the knowledge of initial data at some point of a null hypersurface thus enables one to evaluate the fields at any other relevant point. In the latter case, the analyticity requirement is not strictly necessary, but the fields have to form an IES on real Minkowski space $\mathbb{RM}$, in addition to being well behaved on two-real-dimensional space-like regions provided by intersections between NID hypersurfaces and appropriate light cones.

Actually, there are two types of integral expressions for the elements of an IES. One is the spinning generalization of the Kirchoff–D'Adhemar integrals for massless scalar fields proposed by Penrose [3, 4]. The Kirchoff–D'Adhemar–Penrose (KAP) field integrals can be thought of as being linearly composed of proper Lorentz invariant distributional pieces whenever the initial data for the fields are specified on a null cone. Their integrands are scaling invariant (SI) two-forms on two-spheres which play a very important role in the null description of scattering processes. The field integrals of the other type arise in situations which involve also integrations along null geodesics of $\mathbb{RM}$. These latter field expressions carry SI three-volume forms, and appear as explicit convolutions taken over NID hypersurfaces. Such features afford us an invariant method for treating IES's of interacting fields in a systematic way. The main procedure consists in splitting the fields into an infinite number of elementary distributional contributions that satisfy symbolic field density equations (FDE) on the interior of the closure of the data cone, which are essentially of the same form as those controlling the propagation of the system of interest. Towards achieving the recovery of the entire fields, we have first to set up general prescriptions whereby an

elementary field of arbitrary order may be explicitly calculated, and then to add appropriately all the pieces together. When scattering processes are effectively allowed for, the outgoing fields appear as SI expressions which generally involve both types of field integrals. Under these circumstances, the elementary pieces propagate for a while as massless free fields, but scatter off each other at interior points. Each of the scattering integrals of any order involves a KAP-differential form defined at the point at which the process giving rise to the respective outgoing field happens along with SI volume-forms which take into account the NID contributions coming from all the other relevant points. The NID hypersurfaces for higher-order processes are thus defined as portions of light cones of adequate interior points. Both the charge and the helicity of the incoming fields are preserved when electromagnetic scattering processes are considered alone. Hence, in the case of either integral pattern, the normal and tangential derivatives which are usually required in the space-like framework are combined and made into directional ones defined along generators of NID hypersurfaces. It can, therefore, be said that the geodesics forming NID hypersurfaces appear to play a double role. In effect, they first pick up the components of the fields which partake of the definition of NID sets. Then they single out those space-time directions in which the derivatives carried by the integral expressions are taken.

The explicit expression for any distributional field can always be looked upon as an integral which is taken over an abstract space of suitably connected null graphs that start at the vertex of the data cone and terminate at a fixed interior point. These graphs are normally equipped with forward spin-basis sets whose elements enter particularly into the definition of the null data producing the field, their end-vertices being taken to coincide with the point at which the contribution in question is to be evaluated. The null data are thus specified at those vertices of graphs at which the differential forms occurring in the field integral are set up. It appears that the expression for the null datum for any scattering process explicitly carries only the internal edges of the relevant graphs. Furthermore, the spin-inner-product structures arising from carrying through the corresponding calculations lead automatically to an unambiguous vertex configuration for each graph whence all the processes turn out to be specified by the edge-vertex structures of the scattering diagrams. The information about the null data for the processes appear to be totally carried by suitably contracted first derivatives of the elements of the spin bases.

These null methods were used earlier [5–7] for describing completely the process of mass scattering of classical Dirac fields in IRM. The implementation of standard techniques was based upon the fact that the Van der Waarden form of the Dirac equation [8–11] allows one to treat the Dirac pair

as an IES of massive interacting fields, with the rest-mass playing effectively the role of a coupling constant. Each of the entire fields was given as the sum of two infinite series of terms [7] which were expressed as manifestly finite SI integrals taken over (compact) spaces of null zigzags in $\mathbb{RM}$carrying adequate edge-vertex structures. The formal simplicity of the resulting scattering formulae was due to the choice of the future null cone $\mathcal{C}_0^+$ of an origin O of $\mathbb{RM}$ as the NID hypersurface for the elementary fields. Owing to the possibility of labelling the distributional contributions in a linear way, all the stages of the calculations yielding the null data for the processes were carried out straightforwardly. Nevertheless, for an arbitrary IES it is not generally possible to label the elements of its associated infinite set in this way. For such a system, we have to build up a colored-graph label device which enables us to actually work out the basic prescriptions in a consistent manner. Indeed, this procedure not only makes the whole description more transparent even in cases where the distributional pieces may be labelled linearly, but can also be regarded as a characteristic part of the techniques. In any case, the structure of the colored-vertex configurations seems to be deeply connected with the structure of the pertinent FDE.

This paper is primarily concerned with the presentation of a null description of the dynamics of classical Maxwell–Dirac fields in $\mathbb{RM}$. It can be considered as another non-trivial generalization of the methods introduced by Penrose in connection with the application of NID techniques to IES's (see Ref. [3]). A somewhat important property of this system is that, in order to recover the complete set it suffices to construct the prescriptions for evaluating a finite number of basic null structures. Such configurations are clearly suggested by the pattern of the field equations along with the properties of the proper Lorentz invariant distributional splitting of KAP-integrals [3, 4, 7]. Any element of the entire set can then be recovered by adding together an infinite number of contributions which are obtained by adequately combing these basic blocks together. The FDE are set upon the interior $\mathbb{V}_0^+$ of the closure of $\mathcal{C}_0^+$ whereupon the NID generating all the elementary field contributions are specified. Each distributional piece is represented as a colored tree which is completely specified by the solution of the corresponding density equation. In the case of the potential contributions, the prescriptions for building up the colored graphs lead to patterns which are somewhat different from those of the trees labelling the fields. To any order, this result appears to be directly related to the structure of the solutions of the potential density equations which really give rise to the presence of null loops in the associated Minkowskian configurations. These solutions do not entail any "reduction" of the graphical calculational devices used for evaluating the relevant null structures. The colored graphs turn out to be associated with SI finite integrals which are taken over spaces of

forked and crossed null zigzags that start at O and terminate at a fixed point lying in $\mathbb{V}_0^+$. Our work is organized as follows: Section 2 deals with some of the concepts involved in the two-spinor formulation of the theory [11], and introduces the relevant density equations along with a set of colored-graph rules. Section 3 is concerned with the evaluation of the basic electromagnetic null graphs. In Section 4 the diagrams that describe the processes of electromagnetic scattering of Dirac fields are explicitly calculated. There, the description of pure mass-scattering processes does not play any crucial role, and will therefore be omitted. Some remarks on the structure of the field formulae are made in Section 5. The Lorentz gauge has to be chosen to ensure the exactness of the entire set [3], and is thus taken up from the beginning. At this stage, the actual derivation of the exactness relations for the system [12] will not be presented. The detailed outline of Section 2 through 4 will be given in due course. Throughout the work, use is made of the two-spinor conventions given in Ref. [3]. The natural system of units wherein $c = \hbar = 1$ will also be utilized. Unprimed and primed fields will be referred to as left-handed and right-handed fields, respectively. It must be emphasized, however, that the elementary contributions recovering the complete IES are generally non-analytic. Whence there will be no attempt herein to attribute any specific positive–negative frequency character to the fields. The usual definition of the charge-helicity conjugation operator is adopted, but with the handedness of each of the Dirac fields being reversed under the action of the conjugation. In addition to facilitating the construction of the calculational devices, this requirement enhances some of the features of the diagrams of Section 4. Thus, the fields will be assumed to propagate to the future. The behaviour of null data at the vertex of $\mathcal{C}_0^+$ is discussed extensively by Penrose and Rindler [3]. Here no analycity assumption will be explicitly made, but the elements of the basic NID set are required to be smooth functions at O. The relevance of the work lies in the fact that it affords a concrete background to the construction of a manifestly null quantum electrodynamics. In particular, we believe that such a reformulation would enable one to set up a divergence-free framework for calculating scattering amplitudes. It is upon this belief that the original motivation for elaborating the work rests.

2. Maxwell–Dirac sets

The main aim of this section is to set up a framework which shall be used later to obtain the prescriptions for evaluating the basic Minkowskian structures. In subsection 2.1, we present a review of some facts concerning the two-spinor formulation of the Maxwell–Dirac theory without working out the pertinent variational principle explicitly [11]. The choice of $\mathcal{C}_0^+$

as the NID hypersurface for all the distributional contributions yields a particularly simple set of elementary NID for the system. We utilize the same data set as that suggested in Ref. [3] to define the relevant $\hat{\pi}$-NID (subsection 2.2). These latter data involve certain spin operators which appear to be closely related to the conformally invariant form of the Penrose p-operators [2–4]. Their relevance stems from the fact that they are the data which enter into any SI volume- and KAP-integral expressions. The symbolic density equations associated with the basic null configurations are introduced in subsection 2.3. In subsection 2.4, the rules for building up a set of colored graphs that label the elementary pieces are explained. Nevertheless, the complete specification of the graphs will be achieved in Sections 3 and 4.

Here, as elsewhere, we make use of the convention according to which the unprimed (primed) basis spinor that "enters" a vertex of some null configuration carries an over-script (under-script) which appears as the kernel letter denoting the vertex. The labels for spinors whose flag poles are defined along crossing edges are taken to be the ones for the end-vertices of the relevant subgraphs.

2.1. Maxwell–Dirac theory

A Maxwell–Dirac system in $\mathbb{RM}$ is defined by the set

$$\mathrm{MDS} = \{\phi_{AB}(x),\ \bar{\phi}_{A'B'}(x),\ \Phi_{AA'}(x),\ \psi_A(x),\ \chi_{A'}(x)\}\,. \tag{2.1}$$

In this set, the conjugate quantities $\phi_{AB}(x)$, $\bar{\phi}_{A'B'}(x)$ are the so-called Maxwell spinors. They are both symmetric and normally taken to be dependent opposite-helicity massless uncharged fields of spin$\pm$1. Either of them describes completely [3] the six electromagnetic degrees of freedom at every $x^{AA'} \in \mathbb{RM}$. The vector $\Phi_{AA'}(x)$ is the electromagnetic potential. It is real and usually enters into the definition of the Maxwell bivector $F_{ab}(x)$ as

$$F_{AA'BB'}(x) = 2\nabla_{[AA'}\Phi_{BB']}(x)\,, \tag{2.2}$$

where $\nabla_{AA'}$ is the ordinary partial derivative operator $\partial/\partial x^{AA'}$. The quantities $\psi_A(x)$, $\chi_{A'}(x)$ define the Dirac-field pair [3, 8, 9], and carry locally the information about eight real degrees of freedom. These latter objects are opposite-helicity massive charged spin$\pm$1/2 fields of the same rest-mass and charge. It is useful to define the conjugate pair $\{\bar{\psi}_{A'}(x),\ \bar{\chi}_A(x)\}$ whose elements carry reversed helicities and a charge which is opposite to that carried by the former pair. The conjugation operator, $\hat{\tau}$, is an antilinear involutory mapping which leaves the rest-mass invariant, but it is not here taken to reverse the order of the factors involved in any field expression. It

should be noticed that this assumption appears to agree with the classical character of the fields.

There are twelve (real) gauge-invariant relationships between the Maxwell fields and potential which can be obtained by first splitting the right-hand side of (2.2) into symmetric and skew-symmetric parts involving the index pairs AB and $A'B'$, and then identifying

$$F_{AA'BB'}(x) = \varepsilon_{AB}\bar{\phi}_{A'B'}(x) + \varepsilon_{A'B'}\phi_{AB}(x). \tag{2.3}$$

This procedure yields, in effect,

$$\phi_{AB}(x) = \nabla_{A'(A}\Phi_{B)}^{A'}(x),\ \bar{\phi}_{A'B'}(x) = \nabla_{A(A'}\Phi_{B')}^{A}(x), \tag{2.4}$$

which actually bring out the electromagnetic symmetry property. Clearly, using the Lorentz gauge condition

$$\nabla_{A'[A}\Phi_{B]}^{A'}(x) = 0 \Leftrightarrow \nabla_a\Phi^a(x) = 0 \Leftrightarrow \nabla_{A[A'}\Phi_{B']}^{A}(x) = 0, \tag{2.5}$$

we can drop the symmetrization brackets from the right-hand sides of (2.4) whence Eqs. (2.5) turn out to be re-expressed as

$$\phi_A^A(x) = 0 = \bar{\phi}_{A'}^{A'}(x). \tag{2.6}$$

This simplification is easily accomplished by recalling (2.4) and using the splitting relation

$$\nabla_{A'A}\Phi_B^{A'}(x) = \nabla_{A'(A}\Phi_{B)}^{A'}(x) + \tfrac{1}{2}\varepsilon_{AB}\nabla_c\Phi^c(x), \tag{2.7}$$

along with its complex conjugate. We should stress that the symmetry of the Maxwell fields makes the ordering of the relevant upper and lower indices immaterial. This is the reason why the indices occurring in (2.6) have not been staggered. The structure of the defining expression (2.2) together with the (local) commutativity of the ∇-operators give rise to a set of eight real gauge-invariant identities which constitute the first "half" of Maxwell's equations [3]. These statements can be thought of as constituting the Bianchi identities of the entire theory, and emerge from the simple computation

$$\nabla_{[a}F_{bc]}(x) = \nabla_{[a}\nabla_b\Phi_{c]}(x) = 0 \Rightarrow \nabla^{AA'}{}^*F_{AA'BB'}(x) = 0, \tag{2.8}$$

where ${}^*F_{ab}(x)$ is the dual electromagnetic bivector which is given by

$${}^*F_{AA'BB'}(x) = i[\varepsilon_{AB}\bar{\phi}_{A'B'}(x) - \varepsilon_{A'B'}\phi_{AB}(x)]. \tag{2.9}$$

Explicitly, we have

$$\nabla_B^{A'}\phi^{AB}(x) = \nabla_{B'}^{A}\bar{\phi}^{A'B'}(x)\,, \tag{2.10}$$

which are the identities referred to above.

The part of the complete theory that consists of the second "half" of Maxwell's equations together with the (covariant) Dirac equations arises as the equations of motion involving the following Lagrangian density [11]

$$\mathcal{L}_{\mathrm{MD}} = \mathcal{L}_{\mathrm{M}} + \mathcal{L}_{\mathrm{D}} + \mathcal{L}_{\mathrm{int}}\,, \tag{2.11}$$

where $\mathcal{L}_{\mathrm{M}}$, $\mathcal{L}_{\mathrm{D}}$ and $\mathcal{L}_{\mathrm{int}}$ stand, respectively, for the Maxwell, Dirac and interacting pieces of $\mathcal{L}_{\mathrm{MD}}$ which are written out explicitly as

$$\mathcal{L}_{\mathrm{M}} = \tfrac{1}{8\pi}[\phi_{AB}(x)\phi^{AB}(x) + \bar{\phi}_{A'B'}(x)\bar{\phi}^{A'B'}(x)]\,, \tag{2.12a}$$

$$\begin{aligned}\mathcal{L}_{\mathrm{D}} = i\Big\{ & \tfrac{1}{2}\left[\bar{\chi}_A(x)\nabla^{AA'}\chi_{A'}(x) + \bar{\psi}_{A'}(x)\nabla^{AA'}\psi_A(x)\right] \\ & - \tfrac{1}{2}\left[\left(\nabla^{AA'}\bar{\chi}_A(x)\right)\chi_{A'}(x) + \left(\nabla^{AA'}\bar{\psi}_{A'}(x)\right)\psi_A(x)\right] \\ & - \tfrac{m}{\sqrt{2}}\left[\bar{\chi}_A(x)\psi^A(x) + \bar{\psi}_{A'}(x)\chi^{A'}(x)\right]\Big\}\,,\end{aligned} \tag{2.12b}$$

and

$$\mathcal{L}_{\mathrm{int}} = j_{AA'}(x)\Phi^{AA'}(x)\,, \tag{2.12c}$$

with m denoting the rest-mass of the Dirac fields, and $j_{AA'}(x)$ being a real vector which plays the role of the source for the Maxwell fields and potential. This vector is called the Dirac current density, its explicit expression being written here as

$$j_{AA'}(x) = e\left[\psi_A(x)\bar{\psi}_{A'}(x) + \chi_{A'}(x)\bar{\chi}_A(x)\right]\,, \tag{2.13}$$

where e denotes the charge borne by the elements of the former $\psi\chi$-pair. It should be emphasized that the full Lagrangian density as expressed by (2.11) is a real $\mathrm{SL}(2,\mathbb{C})$-scalar function on $\mathbb{IRM}$. The corresponding equations of motion read

$$\nabla_B^{A'}\frac{\partial\mathcal{L}_{\mathrm{M}}}{\partial\phi_{AB}(x)} + \nabla_{B'}^{A}\frac{\partial\mathcal{L}_{\mathrm{M}}}{\partial\bar{\phi}_{A'B'}(x)} + \frac{\partial\mathcal{L}_{\mathrm{int}}}{\partial\Phi_{AA'}(x)} = 0\,, \tag{2.14a}$$

$$\nabla^{AA'}\frac{\partial\mathcal{L}_{\mathrm{D}}}{\partial\left(\nabla^{AB'}\bar{\psi}_{B'}(x)\right)} - \frac{\partial(\mathcal{L}_{\mathrm{D}} + \mathcal{L}_{\mathrm{int}})}{\partial\bar{\psi}_{A'}(x)} = 0\,, \tag{2.14b}$$

$$\nabla^{AA'}\frac{\partial\mathcal{L}_{\mathrm{D}}}{\partial\left(\nabla^{BA'}\bar{\chi}_B(x)\right)} - \frac{\partial(\mathcal{L}_{\mathrm{D}} + \mathcal{L}_{\mathrm{int}})}{\partial\bar{\chi}_A(x)} = 0\,. \tag{2.14c}$$

Equation (2.14a) gives rise to the second "half" of Maxwell's equations which, when combined with (2.10) and (2.13), yield the gauge-invariant field equations

$$\begin{aligned}\nabla^{B}_{A'}\phi_{AB}(x) &= 2\pi e[\psi_A(x)\bar{\psi}_{A'}(x) + \chi_{A'}(x)\bar{\chi}_A(x)] \\ &= \nabla^{B'}_{A}\bar{\phi}_{A'B'}(x)\,. \end{aligned} \tag{2.15}$$

These statements constitute the Maxwell part of the theory. Equations (2.14b) and (2.14c) yield, in turn, the Dirac equations

$$\mathcal{D}^{AA'}\psi_A(x) = \mu\chi^{A'}(x)\,, \quad \mathcal{D}_{AA'}\chi^{A'}(x) = -\mu\psi_A(x)\,, \tag{2.16}$$

where $\mu = m/\sqrt{2}$, and

$$\mathcal{D}_{AA'} = \nabla_{AA'} - ie\Phi_{AA'}(x)\,. \tag{2.17}$$

The above operator is the covariant derivative operator for the entire theory. For any relevant quantity $\Upsilon^{\mathcal{E}\mathcal{F}'}(x)$, with $\mathcal{E}$ and $\mathcal{F}$ being arbitrary clumped spinor indices, we thus have the commutation relation

$$\begin{aligned}[\mathcal{D}_a, \mathcal{D}_b]\Upsilon^{\mathcal{E}\mathcal{F}'}(x) &= -2ie\left[\nabla_{[a}\left(\Phi_{b]}(x)\Upsilon^{\mathcal{E}\mathcal{F}'}(x)\right) + \Phi_{[a}(x)\nabla_{b]}\Upsilon^{\mathcal{E}\mathcal{F}'}(x)\right] \\ &= -ieF_{ab}(x)\Upsilon^{\mathcal{E}\mathcal{F}'}(x)\,, \end{aligned} \tag{2.18}$$

whence (2.3) can be looked upon as the "curvature" of the theory. It is of some interest to observe that the Bianchi identities (2.8) arise directly from the straightforward computation

$$\begin{aligned}&2\mathcal{D}_{[a}\mathcal{D}_b\mathcal{D}_{c]}\Upsilon^{\mathcal{E}\mathcal{F}'}(x) \\ &= 2\mathcal{D}_{[a}\mathcal{D}_{[b}\mathcal{D}_{c]]}\Upsilon^{\mathcal{E}\mathcal{F}'}(x) \\ &= -ie\mathcal{D}_{[a}\left[F_{bc]}(x)\Upsilon^{\mathcal{E}\mathcal{F}'}(x)\right] \\ &= -ie\left[\left(\nabla_{[a}F_{bc]}\left(\nabla_{[a}F_{bc]}(x)\right)\right)\Upsilon^{\mathcal{E}\mathcal{F}'}(x) + F_{[ab}(x)\mathcal{D}_{c]}\Upsilon^{\mathcal{E}\mathcal{F}'}(x)\right] \\ &= 2\mathcal{D}_{[[a}\mathcal{D}_{b]}\mathcal{D}_{c]}\Upsilon^{\mathcal{E}\mathcal{F}'}(x) \\ &= -ieF_{[ab}(x)\mathcal{D}_{c]}\Upsilon^{\mathcal{E}\mathcal{F}'}(x)\,. \end{aligned} \tag{2.19}$$

One important result emerging from this theory is the conservation of charge. There are several methods of establishing the corresponding statement as an identity [11], but only the one which involves the skew-symmetric operators [3, 11]

$$\blacksquare_{AB} = \mathcal{D}_{A'[A}\mathcal{D}^{A'}_{B]} = \tfrac{1}{2}\epsilon_{AB}\blacksquare\,, \tag{2.20a}$$

$$\blacksquare_{A'B'} = \mathcal{D}_{A[A'}\mathcal{D}^{A}_{B']} = \tfrac{1}{2}\epsilon_{A'B'}\blacksquare\,, \tag{2.20b}$$

with $\blacksquare = \mathcal{D}_c\mathcal{D}^c$, is mentioned here. The basic procedure consists in letting these operators act upon the electromagnetic fields in such a way that the indices carried by the resulting structure are exhausted. After some calculations involving particularly (2.15) and (2.17), we thus obtain

$$\blacksquare_{AB}\phi^{AB}(x) = -2\pi\nabla_{AA'}j^{AA'}(x) = \blacksquare_{A'B'}\bar{\phi}^{A'B'}(x) \equiv 0\,. \tag{2.21}$$

2.2. *Null Initial Data sets*

The simplest NID set on $\mathcal{C}_0^+$ that generates all the fields entering into (2.1) is defined by

$$\text{MDNID} = \{\phi_{L^0}({}^{W}_{o}{}^{A}; W),\ \bar{\phi}_{R^0}(\bar{o}_{W}{}^{A'}; W),\ \psi_L - ({}^{V}_{o}{}^{A}; V),\ \chi_R - (\bar{o}_{U}{}^{A'}; U)\}\,. \tag{2.22}$$

Its elements are explicitly expressed as

$$\phi_{L^0}({}^{W}_{o}{}^{A}; W) = {}^{W}_{o}{}^{A}\,{}^{W}_{o}{}^{B}\phi_{AB}(W),\ \bar{\phi}_{R^0}(\bar{o}_{W}{}^{A'}; W) = \bar{o}_{W}{}^{A'}\,\bar{o}_{W}{}^{B'}\bar{\phi}_{A'B'}(W)\,, \tag{2.23a}$$

$$\psi_L - ({}^{V}_{o}{}^{A}; V) = {}^{V}_{o}{}^{A}\psi_A(V),\ \chi_R - (\bar{o}_{U}{}^{A'}; U) = \bar{o}_{U}{}^{A'}\chi_{A'}(U)\,, \tag{2.23b}$$

with $W^{AA'}$, $V^{AA'}$ and $U^{AA'}$ belonging all to $\mathcal{C}_0^+$. The spinors carried by the arguments of the elements of (2.22) enter into the definition of the (real) flag poles that specify the (null) directions of generators of $\mathcal{C}_0^+$. Each such spinor is chosen to be covariantly constant along the respective generator, the conjugate expressions associated with this choice being (see Eq. (2.26) below)

$${}^{S}_{o}{}^{A}\,\bar{o}_{S}{}^{A'}\frac{\partial\,{}^{S}_{o}{}^{B}}{\partial S^{AA'}} = 0,\ {}^{S}_{o}{}^{A}\,\bar{o}_{S}{}^{A'}\frac{\partial\,\bar{o}_{S}{}^{B'}}{\partial S^{AA'}} = 0\,, \tag{2.24}$$

where the letter S stands for either W, V or U. The data $\phi_{L^0}({}^{W}_{o}{}^{A}; W)$ and $\bar{\phi}_{R^0}(\bar{o}_{W}{}^{A'}; W)$ are, respectively, the (uncharged) left-handed and right-handed electromagnetic null data, whereas $\psi_L - ({}^{V}_{o}{}^{A}; V)$ and $\chi_R - (\bar{o}_{U}{}^{A'}; U)$ are similarly the left-handed and right-handed Dirac null data. These data are spread over the whole of $\mathcal{C}_0^+$, and appear to be formally the same as those for spinning massless free fields [2, 3]. Each of them is a complex-valued scalar function of eight real variables. All the elementary potentials are also generated by them whence there will be no distributional potential contribution arising from potential data on $\mathcal{C}_0^+$. This fact agrees with Penrose's procedure whereby, upon treating the system (2.1), one chooses

a potential-data set whose elements are all taken to vanish on $\mathcal{C}_0^+$ (see Ref. [3]). A further point concerning this procedure will be made in Section 5.

To define the $\hat{\pi}$-NID set, it is convenient to think of $\overset{S}{o}{}^A$ and $\bar{o}_S^{A'}$ as elements of conjugate spin bases $\{\overset{S}{o}{}^A, \overset{K}{o}{}^A\}$, $\{\bar{o}_S^{A'}, \bar{o}_K^{A'}\}$ set up at $S^{AA'}$. The other spinors making up the bases are also taken to be covariantly constant along the generator of the future null cone $\mathcal{C}_S^+$ of $S^{AA'}$ that passes through some point $K^{AA'}$. These latter spinors are chosen in such a way that the flag pole associated with them points in a future null direction through $S^{AA'}$, with the conjugate spin inner products at $S^{AA'}$

$$z_S = \overset{S}{o}{}^A \overset{K}{o}{}_A, \; \bar{z}_S = \bar{o}_S^{A'} \bar{o}_{KA'}, \tag{2.25}$$

being held fixed. Let γ_S denote the generator of $\mathcal{C}_0^+$ through $S^{AA'}$, and r_{0S} be a positive affine parameter on γ_S such that

$$S^{AA'} = r_{0S} \overset{S}{o}{}^A \bar{o}_S^{A'}, \; \mathbb{D}(S;\gamma_S) = \overset{S}{o}{}^A \bar{o}_S^{A'} \frac{\partial}{\partial S^{AA'}}. \tag{2.26}$$

The quantity $\mathbb{D}(S;\gamma_S)$ is the directional derivative operator $\frac{\partial}{\partial r_{0S}}$ at $S^{AA'}$ in the direction of γ_S. Upon acting on the elements of (2.22), the relevant $\hat{\pi}$-operators are defined as follows

$$\begin{aligned} \hat{\pi}_{W1^-} &= \frac{r_{0W}}{(z_W)^2}\{\mathbb{D}(W;\gamma_W) - 3\overset{0}{\rho}(W)\}, \\ \hat{\pi}_{W1^+} &= \frac{r_{0W}}{(\bar{z}_W)^2}\{\mathbb{D}(W;\gamma_W) - 3\overset{0}{\rho}(W)\}, \end{aligned} \tag{2.27}$$

$$\begin{aligned} \hat{\pi}_{V\frac{1}{2}^-} &= \frac{r_{0V}}{z_V}\{\mathbb{D}(V;\gamma_V) - 2\overset{0}{\rho}(V)\}, \\ \hat{\pi}_{U\frac{1}{2}^+} &= \frac{r_{0U}}{\bar{z}_U}\{\mathbb{D}(U;\gamma_U) - 2\overset{0}{\rho}(U)\}, \end{aligned} \tag{2.28}$$

where $\overset{0}{\rho}(S)$ is the (real) convergence of the generators of $\mathcal{C}_0^+$ at $S^{AA'}$ whose defining expression is written as [2, 3, 5, 7]

$$\overset{0}{\rho}(S) = (\overset{S}{o}{}^C \overset{K}{o}{}_C)^{-1} \overset{S}{o}{}_B \overset{K}{o}{}^A \bar{o}_S^{A'} \frac{\partial \overset{S}{o}{}^B}{\partial S^{AA'}}, \tag{2.29}$$

whence $\overset{0}{\rho}(S) = -\frac{1}{r_{OS}}$. We thus have the NID set

$$\hat{\pi}\text{-NID} = \Big\{ \underset{W1^-}{\hat{\pi}}\, \phi_{L^0}(\overset{W}{o}{}^{A}; W),\ \underset{W1^+}{\hat{\pi}}\, \bar{\phi}_{R^0}(\bar{\underset{W}{o}}{}^{A'}; W) \quad \underset{V\frac{1}{2}^-}{\hat{\pi}}\, \psi_{L^-}(\overset{V}{o}{}^{A}; V),\ \underset{U\frac{1}{2}^+}{\hat{\pi}}\, \chi_{R^-}(\bar{\underset{U}{o}}{}^{A'}; U) \Big\}. \tag{2.30}$$

It is worth remarking that, when read from left to right, the data entering into (2.30) appear to be of the types $\{0, -2;\ 0, 0\}$, $\{0, 0;\ -2, 0\}$, $\{0, -1;\ 0, 0\}$ and $\{0, 0;\ -1, 0\}$. At this point, we have made use of the terminology of the compacted spin coefficient formalism of Geroch, Penrose and Held [13], but our complex-conjugation convention involves "reflecting" the number pair occurring on either side of a curly-bracket piece in the vertical that "passes" through the respective semicolon. In fact, the above $\hat{\pi}$-NID constitute a particular version of those used earlier [4, 14] to build up the universal twistorial KAP-integral expressions for massless free fields of arbitrary spin. It is worthwhile to introduce the conjugate Dirac $\hat{\pi}$-data. We have, in effect,

$$\hat{\tau}\ \underset{V\frac{1}{2}^-}{\hat{\pi}}\, \psi_{L^-}(\overset{V}{o}{}^{A}; V) = \underset{V\frac{1}{2}^+}{\hat{\pi}}\, \bar{\psi}_{R^+}(\bar{\underset{V}{o}}{}^{A'}; V), \tag{2.31a}$$

$$\hat{\tau}\ \underset{U\frac{1}{2}^+}{\hat{\pi}}\, \chi_{R^-}(\bar{\underset{U}{o}}{}^{A'}; U) = \underset{U\frac{1}{2}^-}{\hat{\pi}}\, \bar{\chi}_{L^+}(\overset{U}{o}{}^{A}; U). \tag{2.31b}$$

The definition of the elements of (2.30) is illustrated in Fig. 1. The left-handed and right-handed data have been, respectively, denoted by hollow and filled spots bearing suitable charge labels. In what follows, this notation will be also utilized for representing the right-hand sides of Eqs (2.31) diagramatically. In particular, the work of subsection 2.3 involves the specification of Dirac data at points lying on generators of (future) null cones of appropriate points of $\mathbb{V}_0^+$.

2.3. Symbolic density equations

The construction of the formal density equations associated with the elementary field-potential contributions is based only upon the structure of the theory. All the null configurations built up here will be actually used in Sections 3 and 4 as calculational devices for working out the explicit distributional statements. We will see that the reality of the Maxwell fields and potential is lost when the solutions for "higher-order" contributions are obtained. For this reason, another kernel letter will henceforth be used in

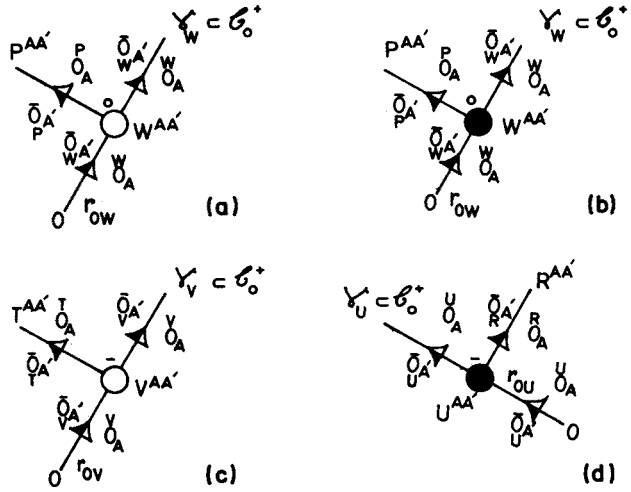

Fig. 1. Diagrams illustrating the definition of the $\hat{\pi}$-data on the future null cone of the origin for the elements of the Maxwell-Dirac set. The left-handed (resp. right-handed) data are shown in (a) and (c) (resp. (b) and (d)) and represented by hollow (resp. filled) spots. The sign carried by the spots refer to the charge borne by the fields involved in the datum expressions.

place of $\bar{\phi}$ to indicate that the left-handed and right-handed electromagnetic fields are generally independent of one another.

For the electromagnetic fields, one has to build up six basic FDE. Two of these involve the (SI) massless free densities $\langle L^0(M);\ \phi_{AB}(x)\rangle$ and $\langle R^0(M);\ \theta_{A'B'}(x)\rangle$ which are produced by electromagnetic data centered at some $M^{AA'} \in \mathcal{C}_0^+$. Such massless free FDE are written at some $x^{AA'}$ lying in the interior of $\mathcal{C}_M^+$ as

$$\nabla^{AA'}\langle L^0(M);\ \phi_{AB}(x)\rangle = 0,\ \nabla^{AA'}\langle R^0(M);\ \theta_{A'B'}(x)\rangle = 0\,. \qquad (2.32)$$

It must be observed that the statements (2.32) are associated with the standard splitting of the KAP-integrals [3, 4, 7] for fields of spin ± 1. This KAP-splitting involves shifting the origin to $M^{AA'}$ in such a way that $x^{AA'}$ appears as a future time-like vector given by the sum of two future null vectors, $r_{MR}\, {}^{M}_{O}{}^{A}\, {}^{\bar{O}}_{M}{}^{A'}$ and $r_{RX}\, {}^{K}_{O}{}^{A}\, {}^{\bar{O}}_{K}{}^{A'}$. The IRM-configurations involved can be readily constructed by adequately transporting the flag poles ${}^{M}_{O}{}^{A}\, {}^{\bar{O}}_{M}{}^{A'}$ and ${}^{K}_{O}{}^{A}\, {}^{\bar{O}}_{K}{}^{A'}$ (see Fig. 2). Hence, $x^{AA'}$ is future-null separated from both $K^{AA'}$ and $R^{AA'}$ which are, in turn, future-null separated from $M^{AA'}$, the point $R^{AA'}$ lying on $\mathcal{C}_0^+$. It should be pointed out that the viability of this

construction rests essentially upon the fact that the field densities entering into (2.32) involve a distributional field [3, 5] whose (non-compact) support is identified with C_M^+. The associated potential densities $\langle L^0(M); \Phi_{AA'}(x)\rangle$ and $\langle R^0(M); \Phi_{AA'}(x)\rangle$ thus satisfy the equations

$$\nabla_{AA'}\langle L^0(M); \Phi_B^{A'}(x)\rangle = \langle L^0(M); \phi_{AB}(x)\rangle$$
$$= \nabla_{AA'}\langle R^0(M); \Phi_B^{A'}(x)\rangle\,, \qquad (2.33a)$$
$$\nabla_{AA'}\langle R^0(M); \Phi_{B'}^{A}(x)\rangle = \langle R^0(M); \theta_{A'B'}(x)\rangle$$
$$= \nabla_{AA'}\langle L^0(M); \Phi_{B'}^{A}(x)\rangle\,. \qquad (2.33b)$$

It will be shown in Section 3 that the solutions of the above equations are the only real electromagnetic densities, whence we have the relationship $\theta = \bar{\phi}$ along with $\langle L^0(M); \Phi_{AA'}(x)\rangle = \langle R^0(M); \Phi_{AA'}(x)\rangle$.

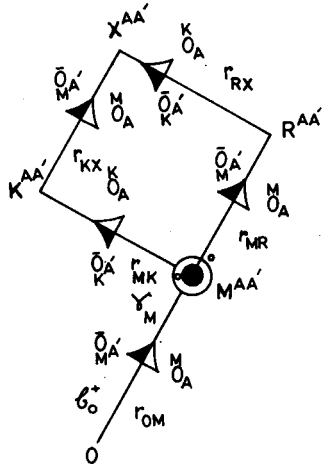

Fig. 2. Planar configuration involved in the standard distributional splitting of the KAP-integrals. The configuration appears as the device for calculating the real electromagnetic densities. In particular the construction entails the affine-parameter equality $r_{MK} = r_{RX}$.

The densities involved in the other electromagnetic FDE are produced by elementary Dirac current pieces of the types $\langle L^- R^+\rangle$ and $\langle R^- L^+\rangle$. The $\hat{\pi}$-data generating such Dirac pieces are centered at points $\{N^{AA'}, P^{AA'}\}$ which lie in either C_0^+ or $\mathbb{V}_0^+$. In this latter case, the Dirac datum spots are actually produced by scattering data. The patterns of the structures involved in the formation of these data are the same as the ones to be constructed in Sections 3 and 4, and will, therefore, be specified later. For simplicity, and without any loss of generality, assume that the data carrying

the same charge are set up at the same point whence the current pieces really appear as $\langle L^-(N)R^+(P)\rangle$ and $\langle R^-(N)L^+(P)\rangle$. The procedure for constructing the relevant null configurations is essentially the same as that giving rise to Fig. 2 since the fields emanating from $N^{AA'}$ and $P^{AA'}$ have once again to be split into their KAP-distributional components. Let $Z^{AA'}$ and $T^{AA'}$ be points lying on $\mathcal{C}_N^+$ and $\mathcal{C}_P^+$, with the corresponding null poles being $\overset{Z}{o}_A \overset{}{\bar{o}}_{A'}$ and $\overset{T}{o}_A \overset{}{\bar{o}}_{A'}$, respectively. The generators γ_Z and γ_T are taken to intersect each other at a "middle" point $M^{AA'}$ while $x^{AA'}$ is now a point lying in the two-plane of $N^{AA'}$, $P^{AA'}$ and $M^{AA'}$ which is future-null separated from both $Z^{AA'}$ and $T^{AA'}$. Thus $x^{AA'}$ belongs to the interior of both $\mathcal{C}_N^+$ and $\mathcal{C}_P^+$, the inner products $z_N = \overset{N}{o}^A \overset{Z}{o}_A$, $z_P = \overset{P}{o}^A \overset{T}{o}_A$ being held fixed together with their complex conjugates, and $z_M = \overset{Z}{o}^A \overset{T}{o}_A$, $\bar{z}_M = \overset{}{\bar{o}}^{A'} \overset{}{\bar{o}}_{A'}$ (see Fig. 3). Invoking (2.15), we then write the symbolic FDE

$$\nabla^B_{A'}\langle L^-(N)R^+(P);\, \phi_{AB}(x)\rangle = 2\pi e\langle L^-(N);\, \psi_A(x)\rangle\langle R^+(P);\, \bar{\psi}_{A'}(x)\rangle$$
$$= \nabla^{B'}_{A}\langle L^-(N)R^+(P);\, \theta_{A'B'}(x)\rangle\,, \quad (2.34)$$

where $\langle L^-(N);\ \psi_A(x)\rangle$ and $\langle R^+(P);\ \bar{\psi}_{A'}(x)\rangle$ denote the conjugate ψ-distributional densities coming from $N^{AA'}$ and $P^{AA'}$, respectively. In a similar way, the FDE for the densities produced by the $\langle R^-(N)L^+(P)\rangle$-piece are written as

$$\nabla^B_{A'}\langle R^-(N)L^+(P);\, \phi_{AB}(x)\rangle = 2\pi e\langle R^-(N);\, \chi_{A'}(x)\rangle\langle L^+(P);\, \bar{\chi}_A(x)\rangle$$
$$= \nabla^{B'}_{A}\langle R^-(N)L^+(P);\, \theta_{A'B'}(x)\rangle\,. \quad (2.35)$$

The potential densities associated with the solutions of Eqs. (2.34) and (2.35) are subject to the equations

$$\nabla_{AA'}\langle L^-(N)R^+(P);\, \Phi^{A'}_B(x)\rangle = \langle L^-(N)R^+(P);\, \phi_{AB}(x)\rangle\,, \quad (2.36a)$$
$$\nabla_{AA'}\langle L^-(N)R^+(P);\, \Phi^{A}_{B'}(x)\rangle = \langle L^-(N)R^+(P);\, \theta_{A'B'}(x)\rangle\,, (2.36b)$$

and

$$\nabla_{AA'}\langle R^-(N)L^+(P);\, \Phi^{A'}_B(x)\rangle = \langle R^-(N)L^+(P);\, \phi_{AB}(x)\rangle\,, \quad (2.37a)$$
$$\nabla_{AA'}\langle R^-(N)L^+(P);\, \Phi^{A}_{B'}(x)\rangle = \langle R^-(N)L^+(P);\, \theta_{A'B'}(x)\rangle\,. (2.37b)$$

A block diagram illustrating the production of the electromagnetic densities is shown in Fig. 4.

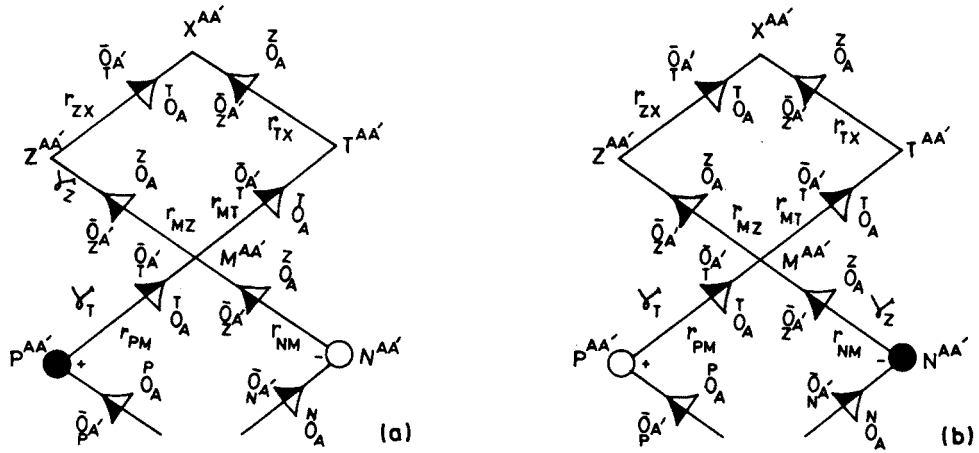

Fig. 3. Null planar configurations associated with the equations for the distributional electromagnetic densities produced by elementary current pieces. The generators of $\mathcal{C}_N^+$ and $\mathcal{C}_P^+$ through $Z^{AA'}$ and $T^{AA'}$ meet at a "middle" point $M^{AA'}$. The point $x^{AA'}$ lies in the plane of $N^{AA'}$, $P^{AA'}$ and $M^{AA'}$, and is defined by transporting parallelly the flag poles $\overset{s}{o}{}^A\,\bar{o}^{A'}_s$ and $\overset{T}{o}{}^A\,\bar{o}^{A'}_T$ along the generators γ_T and γ_Z, respectively. The edges "incoming" at $N^{AA'}$ and $P^{AA'}$ appear in the structures that give rise to the formation of the $\hat{\pi}$-data involved and are not required to lie in the planes of the configurations: (a) (L^-R^+)-structure; (b) (R^-L^+)structure.

When combined with the electromagnetic structures constructed above, the field equations (2.16) give rise to six basic FDE for the Dirac fields. As the entire theory stands, the corresponding statements appear to control the interaction between elementary Dirac fields and electromagnetic potentials. The configurations associated with such FDE can be built up by suitably coupling those of Figs 2 and 3 with the ones corresponding to incoming distributional Dirac fields. It will be seen in Section 4 that this "suitability" is intimately related to the fact that the scattering structures have to carry electromagnetic-field branches which bear the same handedness as that of the incoming and outgoing fields. The procedure leading to this feature amounts to modifying the potential vector kernels associated with the former configurations without violating the relevant FDE, but the former potential poles are indeed recovered when the latter configurations "collapse" so as to restore the former structures. In particular, the handedness feature implies that there are only two appropriate "dual" configurations for each current piece.

The structures under consideration are shown in Figs 5 and 6. In Fig. 5, the incoming fields emanate from $\hat{\pi}$-data set up at a point $D^{AA'}$ which does not, in general, lie on $\mathcal{C}_0^+$, but is taken to belong to the plane spanned by

$M^{AA'}$, $K^{AA'}$ and $x^{AA'}$. One of the generators of $\mathcal{C}_D^+$ lying in this plane contains a point $S^{AA'}$ which is past-null separated from $x^{AA'}$, and thus intersects the geodesic passing through $M^{AA'}$ and $K^{AA'}$ at $m^{AA'}$. At this stage, the affine parameter r_{0M} is not required to lie in the main plane of the configurations. The inner products at $m^{AA'}$ and $D^{AA'}$ are set as $z_m = \overset{S}{o}{}^A \overset{K}{o}{}_A$, $\bar{z}_m = \underset{S}{\bar{o}}{}^{A'} \underset{K}{\bar{o}}{}_{A'}$, and $z_D = \overset{D}{o}{}^A \overset{S}{o}{}_A$, $\bar{z}_D = \underset{D}{\bar{o}}{}^{A'} \underset{S}{\bar{o}}{}_{A'}$.

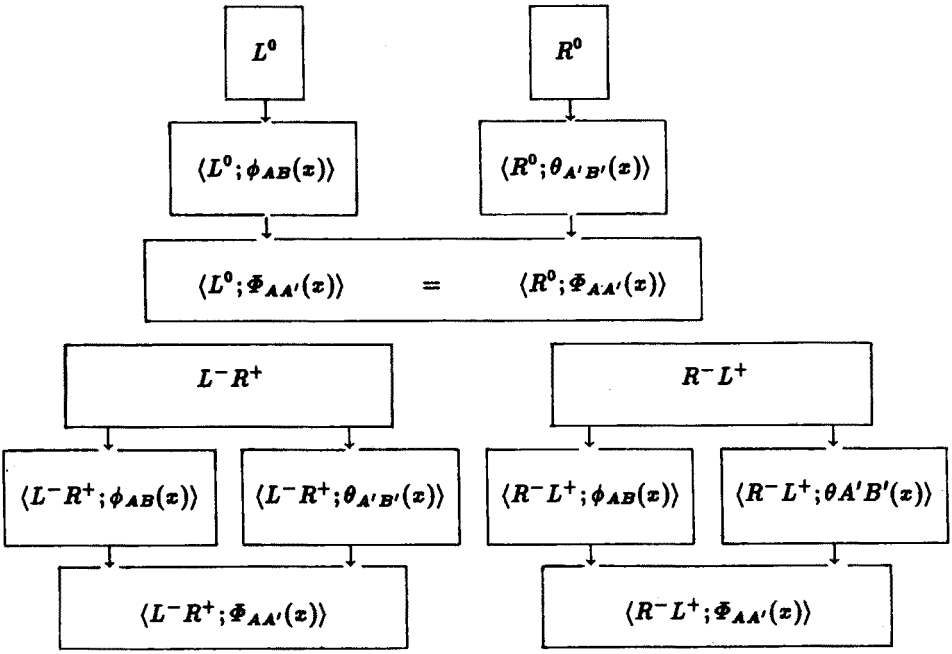

Fig. 4. Block diagram showing the production of the basic electromagnetic densities. For the sake of simplicity some of the vertex arguments have been deleted.

The corresponding FDE are written as follows

$$\nabla^{AA'}\langle L^-(D)L^0(M);\psi_A(x)\rangle = ie\langle L^0(M);\Phi^{AA'}(x)\rangle\langle L^-(D);\psi_A(x)\rangle\,, \tag{2.38}$$

$$\nabla^{AA'}\langle R^-(D)R^0(M);\chi_{A'}(x)\rangle = ie\langle R^0(M);\Phi^{AA'}(x)\rangle\langle R^-(D);\chi_{A'}(x)\rangle\,. \tag{2.39}$$

Operating on these equations with $\nabla^B_{A'}$ and $\nabla^{B'}_A$ and using the Lorentz gauge condition for the potential densities, after some elementary manipulations we obtain the wave equations (with $\Box = \nabla_a\nabla^a$)

$$\Box\langle L^-(D)L^0(M);\psi^A(x)\rangle = -ie\big[\langle L^0(M);\phi^{AB}(x)\rangle\langle L^-(D);\psi_B(x)\rangle - \langle L^0(M);\Phi_B^{A'}(x)\rangle\nabla^{(A}_{A'}\langle L^-(D);\psi^{B)}(x)\rangle\big], \tag{2.40}$$

$$\Box\langle R^-(D)R^0(M);\chi^{A'}(x)\rangle = -ie\big[\langle R^0(M);\theta^{A'B'}(x)\rangle\langle R^-(D);\chi_{B'}(x)\rangle - \langle R^0(M);\Phi_{B'}^{A}(x)\rangle\nabla^{(A'}_{A}\langle R^-(D);\chi^{B')}(x)\rangle\big]. \tag{2.41}$$

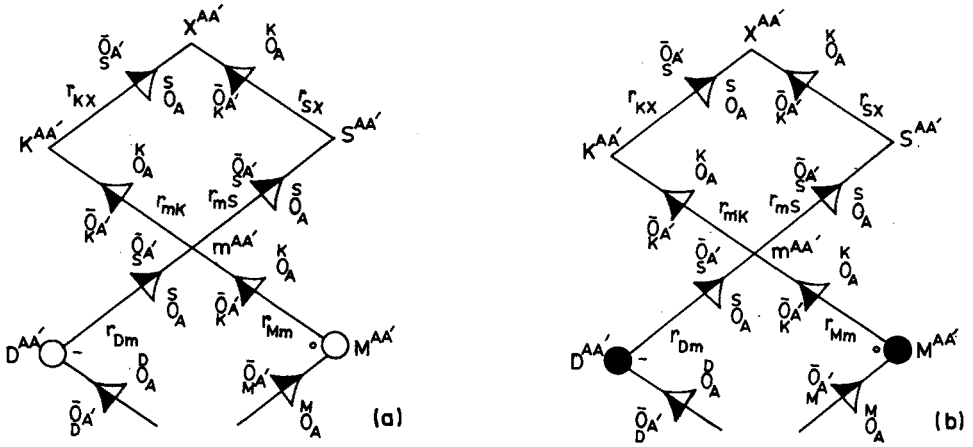

Fig. 5. Planar configurations for the FDE describing the interaction between elementary Dirac densities and "zeroth-order" potential pieces: (a) left-handed structure; (b) right-handed structure.

The construction of Fig. 6 is carried out in a similar way. Now, the scatterer branches involve the current pieces of Fig. 3. The incoming fields are produced by data specified at two points $D^{AA'}$ and $B^{AA'}$, the relevant generators of $\mathcal{C}_D^+$ and $\mathcal{C}_B^+$ intersecting the branches at $F^{AA'}$ and $G^{AA'}$, respectively. In the case of either pair of "dual" structures, the intersection takes place in such a way that these latter points appear to be past-null separated from two points $R^{AA'} \in \mathcal{C}_N^+$ and $K^{AA'} \in \mathcal{C}_P^+$ which lie, therefore, in the planes of $N^{AA'}$, $F^{AA'}$, $D^{AA'}$ and $P^{AA'}$, $G^{AA'}$, $B^{AA'}$, respectively. Furthermore, $x^{AA'}$ lies in both of these planes, and is future-null separated not only from $R^{AA'}$ and $K^{AA'}$, but also from the two other points $\sigma^{AA'} \in$

$\mathcal{C}_D^+$ and $\Sigma^{AA'} \in \mathcal{C}_B^+$ which are, respectively, taken to be future-null separated from $F^{AA'}$ and $G^{AA'}$. The generators of $\mathcal{C}_N^+$ and $\mathcal{C}_P^+$ passing through $R^{AA'}$ and $K^{AA'}$ now meet at $m^{AA'}$, which accordingly belongs to both planes. Evidently, as the configurations stand, the intersection between the two planes is the line passing through $m^{AA'}$ and $x^{AA'}$. The relevant inner products will be defined later (see Eqs (4.21)). For the corresponding FDE, we have

$$\nabla^{AA'}\langle L^-(D)R^+(P)L^-(N);\, \psi_A(x)\rangle$$
$$= ie\langle L^-(N)R^+(P);\, \Phi^{AA'}(x)\rangle\langle L^-(D);\, \psi_A(x)\rangle\,, \tag{2.42}$$

$$\nabla^{AA'}\langle R^-(B)L^-(N)R^+(P);\, \chi_{A'}(x)\rangle$$
$$= ie\langle L^-(N)R^+(P);\, \Phi^{AA'}(x)\rangle\langle R^-(B);\, \chi_{A'}(x)\rangle\,, \tag{2.43}$$

$$\nabla^{AA'}\langle R^-(D)L^+(P)R^-(N);\, \chi_{A'}(x)\rangle$$
$$= ie\langle R^-(N)L^+(P);\, \Phi^{AA'}(x)\rangle\langle R^-(D);\, \chi_{A'}(x)\rangle\,, \tag{2.44}$$

$$\nabla^{AA'}\langle L^-(B)R^-(N)L^+(P);\, \psi_A(x)\rangle$$
$$= ie\langle R^-(N)L^+(P);\, \Phi^{AA'}(x)\rangle\langle L^-(B);\, \psi_A(x)\rangle\,. \tag{2.45}$$

The procedure yielding (2.40) and (2.41) leads also to wave equations associated with Eqs (2.42)–(2.45) which can be immediately obtained from the former statements by replacing L^0 and R^0 by adequate current pieces. For (2.42), for instance, we have

$$\Box\langle L^-(D)R^+(P)L^-(N);\, \psi^A(x)\rangle = -ie\big[\langle L^-(N)R^+(P);\, \phi^{AB}(x)\rangle$$
$$\times\langle L^-(D);\, \psi_B(x)\rangle - \langle L^-(N)R^+(P);\, \Phi_B^{A'}(x)\rangle\nabla^{(A}_{A'}\langle L^-(D);\, \psi^{B)}(x)\rangle\big]\,. \tag{2.46}$$

It should be emphasized that each of the differentiated Dirac densities appearing on the left-hand sides of the equations with which we have been dealing corresponds to an elementary contribution which arises as the result of the interaction between an incoming field and a potential density. Indeed, the solutions of the FDE associated with Eqs (2.16) are to be regarded as densities for new contributions arising in this way. Some block diagrams illustrating these processes are given in Fig. 7. The formation of Dirac datum spots involves appropriately combining configurations that arise from the actual evaluation of the above structures. In accordance with this fact, each contribution will appear as an IRM-integral whose integrand involves the wedge-product of differential forms set up at spotted points.

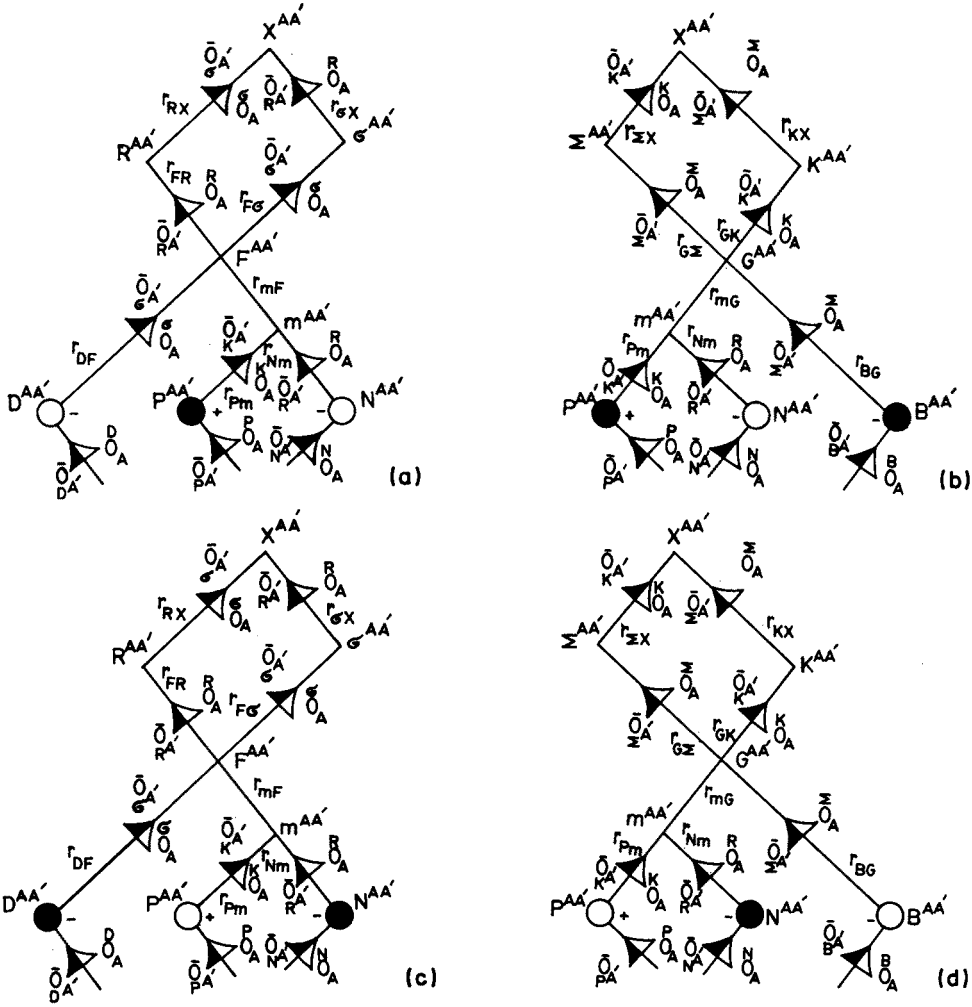

Fig. 6. "Dual" configurations describing the interaction between elementary Dirac and higher-order potential densities. In (a) and (b) (resp. (c) and (d) two Dirac densities propagate in a region with potential produced by a $\psi\bar{\psi}$- (resp. $\chi\bar{\chi}$-) current piece.

2.4. Colored graphs

The distributional pieces which recover each of the elements of (2.1) cannot be labelled in any trivial way. It becomes necessary to design a graphical label device whereby each elementary contribution may be clearly identified. Accordingly, each graph must carry the information about the explicit integral expression associated with a distributional field or a potential. In addition, such a set of graphs must facilitate the construction of the

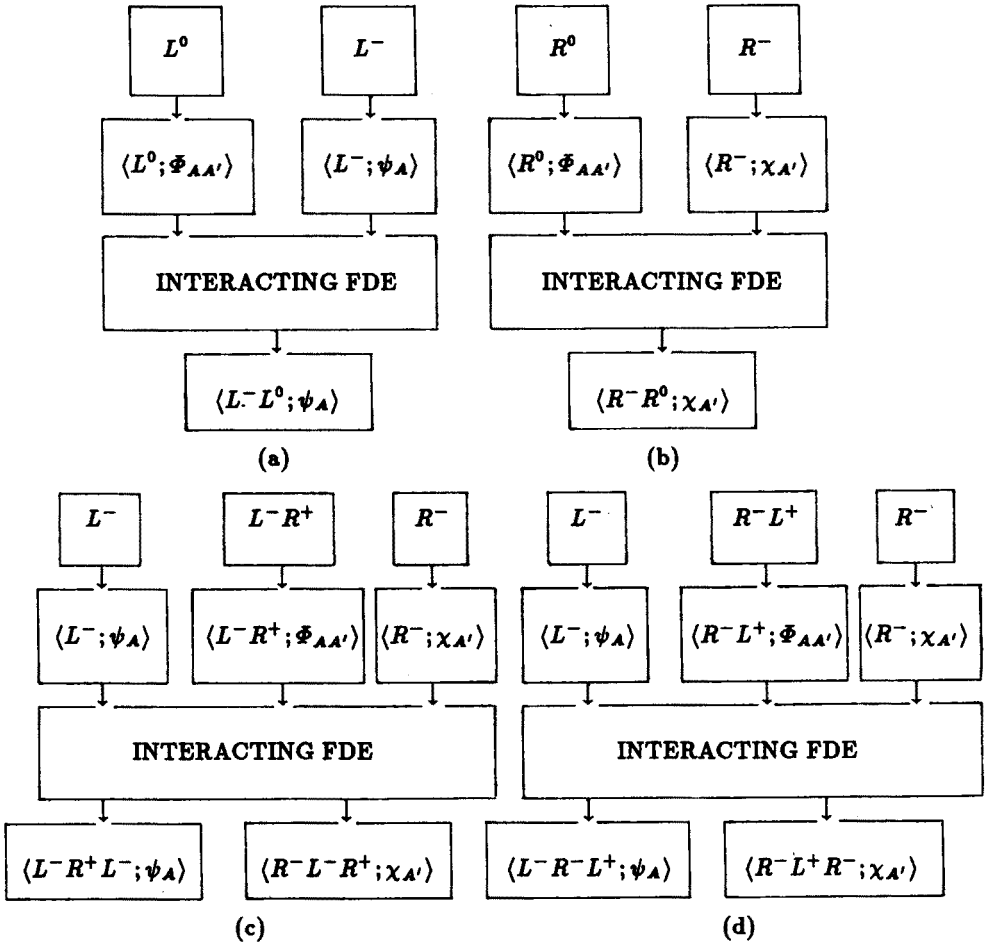

Fig. 7. Block diagram showing how new Dirac fields arise from the interaction between potential and incoming Dirac densities. In (a) and (b) the incoming Dirac densities interact with the "zeroth-order" potential density. In either case the relevant potential piece is produced by the electromagnetic datum that carries the same handedness as the incoming and outgoing fields involved. In (c) and (d) the interaction processes described by the pairs of "dual" configurations are controlled by the FDE of the first order.

integrand of any higher-order contribution. The graphical representation to be built up now also enables one to re-express the mass-scattering zigzag patterns in a simpler manner. This point will be touched upon again in Section 5.

The device used here consists of planar trees which generally carry uncolored and colored vertices connected by solid straight, dashed and wavy

lines. Uncolored vertices bear no meaning at all, but merely appear as endpoints of external lines. Any one of the colored vertices denotes a datum spot. Each of them bears the white color or the black color depending upon whether the corresponding spot is left-handed or right-handed. They always contribute specific differential forms to the integrals, likewise carrying charge labels which effectively remove the charge-helicity ambiguity. Wavy lines appear as external lines starting at colored vertices. Any such line represents a proper Lorentz invariant distributional field [3, 5, 15], and carries a number referring to the "degree" of the distribution. Moreover, all the vertices from which they emanate contribute volume differential forms to the integrands. Each distribution is thus defined with the origin displaced to the IRM-point that corresponds to the vertex bearing the respective line. Colored vertices which do not involve wavy lines contribute KAP-like two-forms, and are always carried by graphs representing explicit outgoing fields. For an arbitrary scattering graph, there is only one vertex of this latter type while all the colored vertices occurring in graphs which do not represent scattering processes are of the former type. Solid straight and dashed lines can be both internal and external. Each of these lines really starts at a colored vertex. Internal dashed lines just play the role of connecting pieces, *not* contributing anything to the integrands. External dashed lines always start at colored vertices which do not correspond to datum spots lying on $\mathcal{C}_0^+$. In this case, each line represents the whole $\hat{\pi}$-datum involved in the formation of the respective IRM-spot. In the other case, the color vertex does not bear such a line, but carries also the contribution due to datum centered at a point of $\mathcal{C}_0^+$ unless it is connected with another colored vertex without bearing a wavy line. Of course, this rule has to be adequately extended when the external dashed lines are replaced by the corresponding subgraphs. In the first instance, if a vertex carries an external dashed line it also carries a wavy line, but the converse is not true in any case. We can, in effect, have vertices carrying wavy lines without bearing external dashed lines and also vertices carrying neither type of line. Thus, a colored vertex which does not carry both external dashed and wavy lines appears as the KAP-vertex of a scattering graph. Notice that this latter rule appears to be particularly relevant when we allow for the "zeroth-order" massless-free-field contributions. Internal solid straight lines connect colored vertices which do not bear necessarily the same color. Each of these lines represents a typical inner-product affine-parameter structure carried by the integrand of an integral expression. In passing, we observe that affine parameters are always carried by denominators of integrands, but inner products are allowed to enter also into numerators. External solid straight lines denote "outgoing" spinors carried by explicit integrands, each spinor being unprimed or primed according to whether the vertex from which the respective line

comes is white or black.

Two vertices of different colors can be "stuck" together to form a double-color vertex. Each such composite vertex bears a wavy line and carries the information associated with a "shrunk" internal solid straight line. It actually appears as one of the colored elements of the vertex-set of a graph, but corresponds to two datum spots of opposite handednesses centered at a common point of $\mathcal{C}_0^+$. Thus, the associated integral contribution involves only the datum whose handedness is the same as that of the spot corresponding to the colored part of the vertex from which the wavy line emanates. As far as our immediate purposes are concerned, such patterns will be used for labelling only the pieces carried by the real potential. For these elementary pieces, it is convenient to attribute an upper-lower end-point character to the external solid straight lines which enables us to decide upon whether the explicitly involved spinors leave or enter the datum spots representing the colored parts. It should be observed that this end-point rule breaks the invariance of the individual pieces when the graphs undergo arbitrary reflections and rotations.

The order of the colored vertices of any graph is irrelevant because the conjugation ambiguity has been eliminated from the beginning. Nevertheless, it seems to be worthwhile to place them in such a way that they bring out the structure of the symbolic expression for the corresponding integral. It appears that, when taken along any edge the sum of the charges equals either zero, $\pm e$ or $\pm 2e$. The values $-e$ and $-2e$ occur in subgraphs which represent conjugate Dirac branches. Explicit colored graphs will be exhibited later in Sections 3 and 4.

3. Evaluation of electromagnetic graphs

In this Section, the explicit evaluation of the basic null diagrams associated with the elementary electromagnetic contributions is carried out. It will be seen that, in the case of the fields, the configurations shown in Figs 2 and 3 turn out to be "reduced" because of the presence of Δ_1-functions in the solutions of the FDE (2.32), (2.34) and (2.35). For the corresponding potential densities, however, the null-loop pattern of the underlying configurations is retained since the solutions of (2.33), (2.36) and (2.37) all involve step functions for the relevant spotted vertices. One important feature of the solutions of the electromagnetic FDE is the correspondence between the handedness of the field densities and that of the datum spots with respect to which the Δ_1-functions are defined. This feature appears to be intimately connected with the structure of the flag poles entering into the solutions for the potential densities. In the particular case of the null configurations of Fig. 3, these latter densities appear essentially as sums of suitably contracted first derivatives of appropriate spinors, which are identified with the

gradient of certain (scalar) functions whose definition comes directly from the structure of the IRM-patterns. Such facts entail a remarkably simple form of the colored trees associated with the integral expressions. The basic procedure for solving the density equations was indeed used earlier for treating pure Dirac fields [5–7]. In essence, it is equivalent to working out the geometric relations for each basic configuration. Subsection 3.1 deals with the construction of the integrals for the fields. In Subsection 3.2 the integral expressions for the potentials are exhibited. Hereafter, a distribution of "degree" k defined with the origin displaced to some point $R^{AA'}$ will be denoted by $\Delta_k(x; R)$.

3.1. Field integrals

As was pointed out previously, the distributional solutions of the free FDE (2.32) constitute the standard SI splitting of the KAP-integrals for fields of spin ± 1. Explicitly, we have [3–6]

$$\langle L^0(M);\, \phi_{AB}(x)\rangle = \frac{1}{2\pi}\, \overset{K}{o}_A\, \overset{K}{o}_B \Delta_1(x; M)\, \underset{M1^-}{\hat{\pi}}\, \phi_{L^0}(\overset{M}{o}{}^C; M), \tag{3.1}$$

$$\langle R^0(M);\, \theta_{A'B'}(x)\rangle = \frac{1}{2\pi}\, \underset{K}{\bar{o}}_{A'}\, \underset{K}{\bar{o}}_{B'} \Delta_1(x; M)\, \underset{M1^+}{\hat{\pi}}\, \bar{\phi}_{R^0}(\underset{M}{\bar{o}}{}^{C'}; M). \tag{3.2}$$

To see how the above solutions actually arise, one has necessarily to derive the expressions for the derivatives of the spinors and affine parameters involved in Fig. 2. We have, in effect

$$x^{AA'} = M^{AA'} + r_{MR}\, \overset{M}{o}_A\, \underset{M}{\bar{o}}_{A'} + r_{RX}\, \overset{K}{o}_A\, \underset{K}{\bar{o}}_{A'}, \tag{3.3}$$

with the point $M^{AA'}$ and the flag pole $\overset{M}{o}_A\, \underset{M}{\bar{o}}_{A'}$ being both held fixed. Thus, differentiating (3.3) and making suitable contractions, we obtain the simple relations

$$\nabla_{AA'}\, \overset{K}{o}_B = -\frac{1}{z_M \bar{z}_M r_{MK}}\, \overset{K}{o}_A\, \underset{M}{\bar{o}}_{A'}\, \overset{M}{o}_B, \tag{3.4}$$

$$\nabla_{AA'} r_{MR} = \frac{1}{z_M \bar{z}_M}\, \overset{K}{o}_A\, \underset{K}{\bar{o}}_{A'}, \quad \nabla_{AA'} r_{RX} = \frac{1}{z_M \bar{z}_M}\, \overset{M}{o}_A\, \underset{M}{\bar{o}}_{A'}, \tag{3.5}$$

together with the conjugate of (3.4). Hence, using the above relations along with the SI distributional expression

$$\nabla_{AA'} \Delta_1(x; M) = r_{RX}\, \overset{K}{o}_A\, \underset{K}{\bar{o}}_{A'} \Delta_2(x; M) - \frac{1}{z_M \bar{z}_M r_{RX}}\, \overset{M}{o}_A\, \underset{M}{\bar{o}}_{A'} \Delta_1(x; M), \tag{3.6}$$

we immediately arrive at Eqs (2.32). The electromagnetic free-field contributions are then written as the conjugate KAP integrals

$$\ll L^0(M);\, \phi_{AB}(x) \gg = \frac{1}{2\pi} \int_{\mathbb{K}}^{1} {}^{X}_{O}{}_{A}\, {}^{X}_{O}{}_{B}\, \hat{\pi}_{M1-}\, \phi_{L^0}({}^{M}_{O}{}^{C};\, M)\, \underset{\sim}{\overset{1}{K}}, \tag{3.7}$$

$$\ll R^0(M);\, \theta_{A'B'}(x) \gg = \frac{1}{2\pi} \int_{\mathbb{K}}^{1} \bar{O}_{X}{}_{A'}\, \bar{O}_{X}{}_{B'}\, \hat{\pi}_{M1+}\, \bar{\phi}_{R^0}(\bar{O}_{M}{}^{C'};\, M)\, \underset{\sim}{\overset{1}{K}}, \tag{3.8}$$

where $\underset{\sim}{\overset{1}{K}}$ is an SI two-form on the space $\overset{1}{\mathbb{K}} \cong S^2$ of null zigzags that start at O and terminate at $x^{AA'}$ (see Ref. [4]). It should be stressed that the Δ_1-function occurring in (3.1) and (3.2) really implies a "reduction" of Fig. 2 so as to make $x^{AA'}$ coincide with $K^{AA'}$. The corresponding graphical representations are depicted as follows

$$\ll L^0(M);\, \phi_{AB}(x) \gg = \bigvee_{O}, \ll R^0(M);\, \theta_{A'B'}(x) \gg = \bigvee_{O}. \tag{3.9}$$

There is an important geometric property of Fig. 3 which arises immediately from the fact that the points $N^{AA'}$ and $P^{AA'}$ are held fixed as $x^{AA'}$ varies suitably. This property amounts to stating that the (real) SI vector

$$K^{AA'} = r_{NM}\, {}^{Z}_{O}{}^{A}\, \bar{O}_{Z}{}^{A'} - r_{PM}\, {}^{T}_{O}{}^{A}\, \bar{O}_{T}{}^{A'}, \tag{3.10}$$

remains constant. Upon transvection with ${}^{N}_{O}{}_{A}\, \bar{O}_{P}{}_{A'}$, we obtain the scalar

$$K = \bar{z}_P({}^{T}_{O}{}^{A}\, {}^{N}_{O}{}_{A}) r_{PM} - z_N(\bar{O}_{Z}{}^{A'}\, \bar{O}_{P}{}_{A'}) r_{NM}, \tag{3.11}$$

which is referred to as the K-scalar for the configurations involved. This scalar quantity will play a significant role in Subsection 3.2 (see also Section 4). The derivatives of the relevant spinors and affine parameters are given by

$$\nabla_{BB'}\, {}^{Z}_{O}{}^{A} = \frac{-r_{PM}}{z_N \bar{z}_M (r_{MZ} r_{MT} - r_{NZ} r_{PT})}\, {}^{Z}_{O}{}_{B}\, \bar{O}_{T}{}_{B'}\, {}^{N}_{O}{}^{A}, \tag{3.12}$$

$$\nabla_{BB'} r_{NZ} = \frac{1}{z_M \bar{z}_M} \left\{ {}^{T}_{O}{}_{B}\, \bar{O}_{T}{}_{B'} + \frac{r_{NZ} r_{PM}}{z_N \bar{z}_N (r_{MZ} r_{MT} - r_{NZ} r_{PT})} \times \left[\bar{z}_N({}^{N}_{O}{}^{A}\, {}^{T}_{O}{}_{A})\, {}^{Z}_{O}{}_{B}\, \bar{O}_{T}{}_{B'} + \text{c.c.} \right] \right\}, \tag{3.13}$$

$$\nabla_{BB'} r_{MZ} = \frac{1}{z_M \bar{z}_M} \left\{ \overset{T}{o}_B \, \underset{T}{\bar{o}}_{B'} + \frac{r_{MZ} r_{PM}}{z_N \bar{z}_N (r_{MZ} r_{MT} - r_{NZ} r_{PT})} \right. \\ \left. \times \left[\bar{z}_N (\overset{N}{o}{}^A \overset{T}{o}_A) \overset{Z}{o}_B \, \underset{T}{\bar{o}}_{B'} + \text{c.c.} \right] \right\}, \tag{3.14}$$

$$\nabla_{BB'} r_{NM} = \frac{1}{z_M \bar{z}_M} \left\{ \frac{r_{NM} r_{PM}}{z_N \bar{z}_N (r_{MZ} r_{MT} - r_{NZ} r_{PT})} \right. \\ \left. \times \left[\bar{z}_N (\overset{N}{o}{}^A \overset{T}{o}_A) \overset{Z}{o}_B \, \underset{T}{\bar{o}}_{B'} + \text{c.c.} \right] \right\}, \tag{3.15}$$

along with the conjugate of (3.12) and the relations which are obtained from those given above by interchanging $N \leftrightarrow P$ and $Z \leftrightarrow T$, the symbol "c.c." standing for "complex conjugate". Notice that the piece involving a difference between products of parameters in the denominators is invariant under these interchanges, which actually include changing the overall sign of (3.12) (see Eqs (3.22) and (3.27)). The entire set of expressions can be derived by differentiating the relations

$$\begin{aligned} x^{AA'} &= N^{AA'} + r_{NZ} \overset{Z}{o}{}^A \underset{Z}{\bar{o}}{}^{A'} + r_{ZX} \overset{T}{o}{}^A \underset{T}{\bar{o}}{}^{A'} \\ &= P^{AA'} + r_{PT} \overset{T}{o}{}^A \underset{T}{\bar{o}}{}^{A'} + r_{TX} \overset{Z}{o}{}^A \underset{Z}{\bar{o}}{}^{A'}, \end{aligned} \tag{3.16}$$

and making appropriate contractions. When deriving these expressions, it is convenient to utilize the trivial affine-parameter identities

$$r_{NZ} r_{PM} + r_{NM} r_{MT} \equiv r_{NM} r_{PT} + r_{MZ} r_{PM} \equiv -(r_{MZ} r_{MT} - r_{NZ} r_{PT}).$$

To write out the middle blocks of Eqs (2.34) and (2.35) explicitly, we use the KAP-splitting relations for the Dirac current densities

$$e\langle L^-(N); \psi_A(x)\rangle \langle R^+(P); \bar{\psi}_{A'}(x)\rangle = \frac{e}{4\pi^2} \langle \overset{Z}{o}_A \Delta_1(x; N) \underset{N\frac{1}{2}^-}{\hat{\pi}} \psi_L - (\overset{N}{o}{}^B; N)\rangle \\ \times \langle \underset{T}{\bar{o}}_{A'} \Delta_1(x; P) \underset{P\frac{1}{2}^+}{\hat{\pi}} \bar{\psi}_R + (\underset{P}{\bar{o}}{}^{B'}; P)\rangle, \tag{3.17}$$

$$e\langle R^-(N); \chi_{A'}(x)\rangle \langle L^+(P); \bar{\chi}_A(x)\rangle = \frac{e}{4\pi^2} \langle \underset{Z}{\bar{o}}_{A'} \Delta_1(x; N) \underset{N\frac{1}{2}^+}{\hat{\pi}} \chi_R - (\underset{N}{\bar{o}}{}^{B'}; N)\rangle \\ \times \langle \overset{T}{o}_A \Delta_1(x; P) \underset{P\frac{1}{2}^-}{\hat{\pi}} \bar{\chi}_L + (\overset{P}{o}{}^B; P)\rangle. \tag{3.18}$$

The procedure for solving the equation occurring in (2.34) that involves the left-handed field density is now developed. We will see that the solutions of the other electromagnetic FDE can at once be achieved by making

adequate replacements. In accordance with the general prescription given in Refs [4–6], one seeks a solution of the form

$$\langle L^-(N)R^+(P);\,\phi_{AB}(x)\rangle = \alpha_A\beta_B\Delta_j(x;\,N)\Delta_k(x;\,P)$$
$$\times \underset{N\frac{1}{2}^-}{\hat{\pi}}\psi_{L^-}(\overset{N}{o}{}^C;\,N)\underset{P\frac{1}{2}^+}{\hat{\pi}}\bar{\psi}_{R^+}(\bar{o}_P^{\,C'};\,P), \tag{3.19}$$

where α_A and β_B are spinors to be determined along with j and k. Thus operating on (3.19) with $\nabla^{BA'}$ and making use of the generalized SI derivative

$$\nabla^{BA'}\Delta_j(x;\,N) = r_{NZ}\overset{Z}{o}{}^B\bar{o}_Z^{\,A'}\Delta_{j+1}(x;\,N) - \frac{j}{z_M\bar{z}_M r_{NZ}}\overset{T}{o}{}^B\bar{o}_T^{\,A'}\Delta_j(x;\,N), \tag{3.20}$$

together with the expression that arises from applying the NP-ZT interchange rule to (3.20), we obtain

$$\alpha_A\beta_B = \lambda\overset{Z}{o}{}_A\overset{Z}{o}{}_B,\ \lambda = \frac{e}{2\pi}\frac{r_{NZ}}{z_M(r_{MZ}r_{MT} - r_{NZ}r_{PT})},\ j=1, k=0. \tag{3.21}$$

Hence the solution sought is uniquely given by

$$\langle L^-(N)R^+(P);\,\phi_{AB}(x)\rangle = \frac{-e}{2\pi z_M r_{PM}}\overset{Z}{o}{}_A\overset{Z}{o}{}_B\Delta_1(x;\,N)\Delta_0(x;\,P)$$
$$\times \underset{N\frac{1}{2}^-}{\hat{\pi}}\psi_{L^-}(\overset{N}{o}{}^C;\,N)\underset{P\frac{1}{2}^+}{\hat{\pi}}\bar{\psi}_{R^+}(\bar{o}_P^{\,C'};\,P), \tag{3.22}$$

provided that

$$\nabla^{BA'}(\lambda\overset{Z}{o}{}_A\overset{Z}{o}{}_B) = -\frac{e}{2\pi}\frac{\overset{Z}{o}{}_A\bar{o}_T^{\,A'}}{z_M\bar{z}_M(r_{MZ}r_{MT} - r_{NZ}r_{PT})}. \tag{3.23}$$

In fact, the terms involving $\Delta_1(x;\,N)$ and $\Delta_0(x;\,P)$ cancel when (3.22) is inserted into the density equation under consideration, the remaining terms thus reinstating the pertinent right-hand side. The field contribution is then symbolically expressed as

$$\ll L^-(N)R^+(P);\,\phi_{AB}(x)\gg$$
$$= \int_{\mathbf{E}_L}\langle L^-(N)R^+(P);\,\phi_{AB}(x)\rangle\,\underset{\sim}{\Delta}_I\wedge\underset{\sim}{\Omega}_{\bar{N}}\wedge\underset{\sim}{\Delta}_{II}\wedge\underset{\sim}{\Omega}_P^+, \tag{3.24}$$

where the (charged) Δ-forms are those associated with the contributions of the spotted vertices occurring in the configurations that give rise to the

formation of the relevant current spots. The Ω-forms are associated with the explicit contributions emanating from $N^{AA'}$ and $P^{AA'}$. These latter forms are SI volume forms of the type

$$\underset{\sim}{\Omega}_W = \frac{dr_{HW}}{r_{HW}} \wedge \overset{W}{\underset{\sim}{S}}, \tag{3.25}$$

where the affine parameter involved lies on the generator of the future null cone of an appropriate vertex $H^{AA'}$ that appears in the underlying configuration, and $\overset{W}{\underset{\sim}{S}}$ stands for an SI element of two-surface area of the (space-like) intersection between $\mathcal{C}_Y^-$ and $\mathcal{C}_H^+$, with $Y^{AA'}$ denoting a suitable point lying to the future of either $N^{AA'}$ or $P^{AA'}$ (see Ref. [7]). The integral is taken over the space $\mathbb{E}_L$ of structures of the type shown in Fig. 8a. Once again, we see clearly that the former calculational structure (Fig. 3a) is "reduced" because of the presence of the distribution $\Delta_1(x; N)$. Thus, for Eq. (3.24), we have the graph

$\ll L^-(N)R^+(P); \phi_{AB}(x) \gg =$

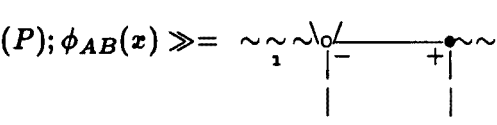

(3.26)

It is evident that the (typical) structure associated with the internal line occurring in the above graph is $\frac{-e/2\pi}{z_M r_{PM}}$.

When worked out explicitly, the prescription yielding (3.26) shows us that the distributional solution for the right-handed density involved in Eqs (2.34) can be obtained from (3.22) by first applying the NP–ZT interchange rule to the affine parameter and distributions, replacing the explicit $\overset{Z}{o}_A$-spinors by $\bar{o}_{A'}$ $\bar{o}_{B'}$, and then taking a complex conjugation of the inner product at $M^{AA'}$, the overall sign being also changed. We thus have the statement

$$\langle L^-(N)R^+(P); \theta_{A'B'}(x)\rangle = \frac{e}{2\pi \bar{z}_M r_{NM}} \bar{o}_{A'} \bar{o}_{B'} \Delta_1(x; P)\Delta_0(x; N)$$
$$\times \underset{N\frac{1}{2}^-}{\hat{\pi}} \psi_{L^-}\left(\overset{N}{o}{}^C; N\right) \underset{P\frac{1}{2}^+}{\hat{\pi}} \bar{\psi}_R + \left(\bar{o}_P{}^{C'}; P\right), \tag{3.27}$$

whence the corresponding contribution is written as

$$\ll L^-(N)R^+(P); \theta_{A'B'}(x) \gg$$
$$= \int_{\mathbf{E}_R} \langle L^-(N)R^+(P); \theta_{A'B'}(x)\rangle \underset{\sim}{\Delta}_I \wedge \underset{\sim}{\Omega}_N^- \wedge \underset{\sim}{\Delta}_{II} \wedge \underset{\sim}{\Omega}_P^+, \tag{3.28}$$

with the integral being taken over the space of null configurations of the type exhibited in Fig. 8b. The colored-graph representation of Eq. (3.28) is then given by

$$\ll L^{-}(N)R^{+}(P); \theta_{A'B'}(x) \gg =$$ 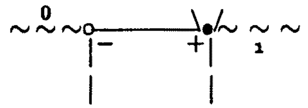 (3.29)

To the FDE (2.35) with the current density (3.18), the standard prescription yields the solutions

$$\langle R^{-}(N)L^{+}(P);\ \phi_{AB}(x)\rangle = \frac{e}{2\pi z_{M^{\tau}NM}} \overset{T}{o}{}_{A} \overset{T}{o}{}_{B} \Delta_1(x;\ P)\Delta_0(x;\ N)$$
$$\times \underset{N\frac{1}{2}^{+}}{\hat{\pi}} \chi_{R^{-}}\left(\underset{N}{\bar{o}}{}^{C'};\ N\right) \underset{P\frac{1}{2}^{-}}{\hat{\pi}} \bar{\chi}_{L^{+}}\left(\overset{P}{o}{}^{C};\ P\right), \qquad (3.30)$$

$$\langle R^{-}(N)L^{+}(P);\ \theta_{A'B'}(x)\rangle = -\frac{e}{2\pi \bar{z}_{M^{\tau}PM}} \underset{Z}{\bar{o}}{}_{A'} \underset{Z}{\bar{o}}{}_{B'} \Delta_1(x;\ N)\Delta_0(x;\ P)$$
$$\times \underset{N\frac{1}{2}^{+}}{\hat{\pi}} \chi_{R^{-}}\left(\underset{N}{\bar{o}}{}^{C'};\ N\right) \underset{P\frac{1}{2}^{-}}{\hat{\pi}} \bar{\chi}_{L^{+}}\left(\overset{P}{o}{}^{C};\ P\right). \qquad (3.31)$$

The associated field integrals are thus expressed as

$$\ll R^{-}(N)L^{+}(P);\ \phi_{AB}(x) \gg$$
$$= \int_{\mathcal{E}_L} \langle R^{-}(N)L^{+}(P);\ \phi_{AB}(x)\rangle\, \underset{\sim}{\delta}_{I} \wedge \underset{\sim}{\Omega}{}^{-}_{N} \wedge \underset{\sim}{\delta}_{II} \wedge \underset{\sim}{\Omega}{}^{+}_{P}, \qquad (3.32)$$

$$\ll R^{-}(N)L^{+}(P);\ \theta_{A'B'}(x) \gg$$
$$= \int_{\mathcal{E}_R} \langle R^{-}(N)L^{+}(P);\ \theta_{A'B'}(x)\rangle\, \underset{\sim}{\delta}_{I} \wedge \underset{\sim}{\Omega}{}^{-}_{N} \wedge \underset{\sim}{\delta}_{II} \wedge \underset{\sim}{\Omega}{}^{+}_{P}, \qquad (3.33)$$

with the differential forms bearing essentially the same meaning as in (3.24) and (3.28). We notice that the integrands of Eqs (3.32) and (3.33) can be constructed from (3.22) and (3.27) by using the NP–ZT rule and supplying the $\hat{\pi}$-data. The configurations which are relevant for the integrations are depicted in Figs 8c and 8d. Accordingly, a simple white-black interchange rule yields the graphical representations

$$\ll R^{-}(N)L^{+}(P); \phi_{AB}(x) \gg =$$ 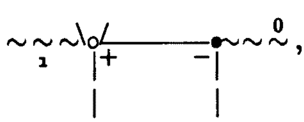 (3.34)

$$\ll R^{-}(N)L^{+}(P);\theta_{A'B'}(x) \gg =$$

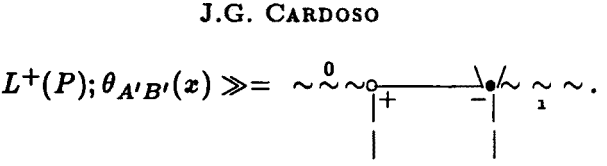

(3.35)

It should be emphasized that the Δ_1-function "reduction" yielding the patterns of Fig. 8 implies in each case the identification of $x^{AA'}$ with either $Z^{AA'}$ or $T^{AA'}$.

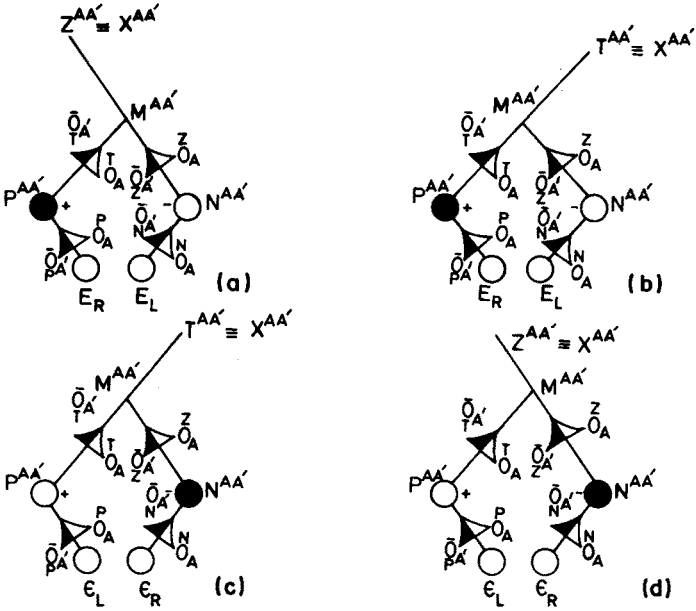

Fig. 8. Null configurations involved in the integrations leading to the basic electromagnetic-field contributions produced by current pieces. The loops denote the branches that give rise to the formation of the current datum spots. The structures for left-handed (resp. right-handed) fields are shown in (a) and (c) (resp. (b) and (d)). In any case the relevant diagram has to be suitably displaced so as to make its end-vertex coincide with $x^{AA'}$.

3.2. Potential integrals

Upon working out the prescription for obtaining the basic potential expressions, one has to solve simultaneously the density equations that enter into each of the pairs (2.33), (2.36) and (2.37). The explicit form of Eqs (2.33) is achieved by simply using the field densities (3.1) and (3.2). We thus have

$$\nabla_{AA'}\langle L^0(M);\Phi_B^{A'}(x)\rangle = \frac{1}{2\pi}\,{}^{K}_{O}{}_{A}\,{}^{K}_{O}{}_{B}\Delta_1(x;M)\,\hat{\pi}_{M1^-}\,\phi_{L^0}\left({}^{M}_{O}{}^{C};M\right),\quad(3.36)$$

$$\nabla_{AA'}\langle R^0(M);\Phi^A_{B'}(x)\rangle = \frac{1}{2\pi}\,\bar{o}_K^{\,A'}\,\bar{o}_K^{\,B'}\Delta_1(x;M)\,\hat{\pi}_{M1+}\,\bar{\phi}_{R^0}(\bar{o}_M^{\,C'};M). \tag{3.37}$$

It follows that, invoking the basic procedure of which we made use in the preceding subsection and employing the formulae (3.4)–(3.6), we obtain the expression

$$\begin{aligned}\langle L^0(M);\,\Phi_{AA'}(x)\rangle &= \frac{1}{2\pi}\left[\frac{1}{\bar{z}_M r_{RX}}\Delta_0(x;M)\,o^K_A\,\bar{o}^{\,A'}_M\,\hat{\pi}_{M1-}\,\phi_{L^0}(o^M_C;M)+\text{c.c.}\right]\\ &= \langle R^0(M);\,\Phi_{AA'}(x)\rangle\,.\end{aligned} \tag{3.38}$$

This is the real ("zeroth order") potential density referred to before. Notice that it can be re-expressed as

$$\begin{aligned}\langle L^0(M);\,\Phi_{AA'}(x)\rangle &= \frac{1}{2\pi}\left[\Delta_0(x;M)\,o^K_B\nabla_{AA'}\,o^K_B\,\hat{\pi}_{M1-}\,\phi_{L^0}(o^M_C;M)+\text{c.c.}\right]\\ &= \langle R^0(M);\,\Phi_{AA'}(x)\rangle\,.\end{aligned} \tag{3.39}$$

The corresponding SI contribution is then written as

$$\ll L^0(M);\Phi_{AA'}(x)\gg = \int_{\mathcal{G}_5}\langle\mathcal{H}^0(M);\Phi_{AA'}(x)\rangle\,\underset{\sim}{\Omega}{}^0_M = \ll R^0(M);\Phi_{AA'}(x)\gg, \tag{3.40}$$

where the letter $\mathcal{H}$ stands for either L or R, and the (five-edge) configurations over which the integral is taken are of the type shown in Fig. 9. We should point out that the presence of the step function in (3.39) does not entail any collapse of the null loop of Fig. 2. The graphical representation of Eq. (3.40) is thus depicted as follows

$\ll L^0(M);\Phi_{AA'}(x)\gg =$ 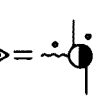 $+$ 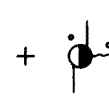 $= \ll R^0(M);\Phi_{AA'}(x)\gg$. (3.41)

Recall that, for the potential contribution just calculated, it is convenient to use the upper-lower end-point convention. In fact, the conjugate graphical pieces carried by Eqs (3.41) can be easily constructed from one another by reflecting the spinor lines in the verticals that "contain" the "interfaces" between the colored parts, keeping the vertices fixed.

To calculate the potential density that enters into Eqs (2.36), it is convenient (but not strictly necessary) to use the whole expression for $\alpha_A\beta_B$ as

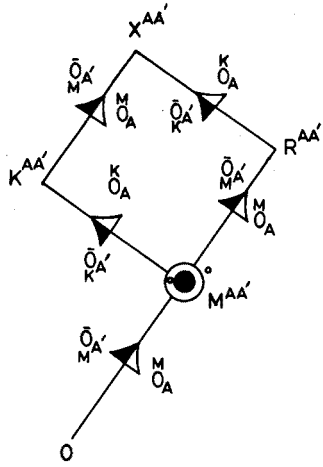

Fig. 9. Five-edge null configuration involved in the integration of the real potential density. The presence of a step function in the overall integrand does not entail any collapse of the null loop.

given by (3.21) in conjuction with the one associated with the right-handed field density (3.27). We thus have the explicit statements

$$\nabla_{AA'}\langle L^-(N)R^+(P);\,\Phi_B^{A'}(x)\rangle = \frac{e}{2\pi}\frac{r_{NZ}\Delta_1(x;N)\Delta_0(x;P)}{z_M(r_{MZ}r_{MT}-r_{NZ}r_{PT})}\,{}^{z}_{o}{}_{A}\,{}^{z}_{o}{}_{B}$$
$$\times \underset{N\frac{1}{2}^-}{\hat{\pi}}\psi_{L^-}({}^{N}_{o}{}^{C};N)\underset{P\frac{1}{2}^+}{\hat{\pi}}\bar{\psi}_R+({}^{\bar{o}}_{P}{}^{C'};P)\,, \qquad (3.42)$$

and

$$\nabla_{AA'}\langle L^-(N)R^+(P);\,\Phi^A_{B'}(x)\rangle = -\frac{e}{2\pi}\frac{r_{PT}\Delta_1(x;P)\Delta_0(x;N)}{\bar{z}_M(r_{MZ}r_{MT}-r_{NZ}r_{PT})}\,{}^{\bar{o}}_{T}{}_{A'}\,{}^{\bar{o}}_{T}{}_{B'}$$
$$\times \underset{N\frac{1}{2}^-}{\hat{\pi}}\psi_{L^-}({}^{N}_{o}{}^{C};N)\underset{P\frac{1}{2}^+}{\hat{\pi}}\bar{\psi}_R+({}^{\bar{o}}_{P}{}^{C'};P)\,. \qquad (3.43)$$

Therefore, when inserted into (3.42) and (3.43), a common solution of the form

$$\langle L^-(N)R^+(P);\Phi_{AA'}(x)\rangle = \mu\xi_A\eta_{A'}\Delta_j(x;P)\Delta_k(x;N)$$
$$\times \underset{N\frac{1}{2}^-}{\hat{\pi}}\psi_L-({}^{N}_{o}{}^{C};N)\underset{P\frac{1}{2}^+}{\hat{\pi}}\bar{\psi}_R+({}^{\bar{o}}_{P}{}^{C'};P)\,, \qquad (3.44)$$

leads us uniquely to

$$\mu = -\frac{e}{2\pi}\frac{1}{z_M\bar{z}_M(r_{MZ}r_{MT}-r_{NZ}r_{PT})}\,,\quad \xi_A\eta_{A'} = {}^{z}_{o}{}_{A}\,{}^{\bar{o}}_{T}{}_{A'}\,,\quad j=k=0\,, \qquad (3.45)$$

where the relation (3.20) and its NP–ZT dual have been used. It follows that the pertinent potential contribution is written as

$$\ll L^-(N)R^+(P);\Phi_{AA'}(x)\gg= \int\limits_{\mathcal{E}_{\psi\bar{\psi}}} \langle L^-(N)R^+(P);\Phi_{AA'}(x)\rangle \underset{\sim}{\Delta}_I \wedge \underset{\sim}{\Omega}^-_N \wedge \underset{\sim}{\Delta}_{II} \wedge \underset{\sim}{\Omega}^+_P, \tag{3.46}$$

with the (SI) density involved being explicitly given by

$$\langle L^-(N)R^+(P);\Phi_{AA'}(x)\rangle = -\frac{e}{2\pi}\frac{\overset{Z}{o}{}_A\,\underset{T}{\bar{o}}_{A'}\Delta_0(x;P)\Delta_0(x;N)}{z_M\bar{z}_M(r_{MZ}r_{MT}-r_{NZ}r_{PT})} \times \underset{N\frac{1}{2}^-}{\hat{\pi}}\psi_L\text{-}(\overset{N}{o}{}^C;N)\underset{P\frac{1}{2}^+}{\hat{\pi}}\bar{\psi}_R+(\underset{P}{\bar{o}}{}^{C'};P). \tag{3.47}$$

The integral (3.46) is taken over the space $\mathcal{E}_{\psi\bar{\psi}}$ of null patterns of the type exhibited in Fig. 10a, its graphical representation being

$\ll L^-(N)R^+(P);\phi_{AA'}(x)\gg=$ 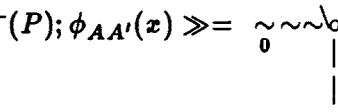 . (3.48)

Thus, for the structure (3.48), the internal line represents the factor

$$-e/2\pi z_M\bar{z}_M(r_{MZ}r_{MT}-r_{NZ}r_{PT}).$$

In verifying that (3.47) does indeed satisfy Eqs (3.42) and (3.43), one can make use of the relations

$$\nabla_{AA'}[z_M\bar{z}_M(r_{MZ}r_{MT}-r_{NZ}r_{PT})] = -(r_{NM}\overset{Z}{o}{}_A\,\underset{Z}{\bar{o}}_{A'}+r_{PM}\overset{T}{o}{}_A\,\underset{T}{\bar{o}}_{A'}), \tag{3.49}$$

and

$$\begin{aligned}&\nabla_{BB'}[\overset{Z}{o}{}^A\,\underset{T}{\bar{o}}{}^{A'}\Delta_0(x;P)\Delta_0(x;N)]\\ &=(z_N\bar{z}_Mr_{NM}\overset{Z}{o}{}^A\,\underset{P}{\bar{o}}{}^{A'}-z_M\bar{z}_Pr_{PM}\overset{N}{o}{}^A\,\underset{T}{\bar{o}}{}^{A'})\\ &\times\frac{\overset{Z}{o}{}_B\,\underset{T}{\bar{o}}_{B'}\Delta_0(x;P)\Delta_0(x;N)}{z_Nz_M\bar{z}_M\bar{z}_P(r_{MZ}r_{MT}-r_{NZ}r_{PT})}+\Big[r_{NZ}\overset{Z}{o}{}_B\,\underset{Z}{\bar{o}}_{B'}\Delta_1(x;N)\Delta_0(x;P)\\ &+r_{PT}\overset{T}{o}{}_B\,\underset{T}{\bar{o}}_{B'}\Delta_1(x;P)\Delta_0(x;N)\Big]\overset{Z}{o}{}^A\,\underset{T}{\bar{o}}{}^{A'},\end{aligned} \tag{3.50}$$

which actually imply that

$$
\begin{aligned}
&\nabla_{BB'}\langle L^-(N)R^+(P);\Phi_{AA'}(x)\rangle = \\
&-\frac{e}{2\pi}\Bigg\{\Delta_0(x;N)\Delta_0(x;P)\Bigg[\Bigg(\frac{\bar z_M r_{NM}\overset{Z}{o}_A\underset{P}{\bar o}_{A'}}{\bar z_P}-\frac{z_M r_{PM}\overset{N}{o}_A\underset{T}{\bar o}_{A'}}{z_N}\Bigg)\overset{Z}{o}_B\underset{T}{\bar o}_{B'} \\
&+\big(r_{NM}\overset{Z}{o}_B\underset{Z}{\bar o}_{B'}+r_{PM}\overset{T}{o}_B\underset{T}{\bar o}_{B'}\big)\overset{Z}{o}_A\underset{T}{\bar o}_{A'}\Bigg]+z_M\bar z_M(r_{MZ}r_{MT}-r_{NZ}r_{PT}) \\
&\times\big[r_{NZ}\overset{Z}{o}_B\underset{Z}{\bar o}_{B'}\Delta_1(x;N)\Delta_0(x;P)+r_{PT}\overset{T}{o}_B\underset{T}{\bar o}_{B'}\Delta_1(x;P)\Delta_0(x;N)\big]\overset{Z}{o}_A\underset{T}{\bar o}_{A'}\Bigg\} \\
&\times\frac{\underset{N\frac12^-}{\hat\pi}\;\psi_{L^-}(\overset{N}{o}^C;N)\;\underset{P\frac12^+}{\hat\pi}\;\bar\psi_{R^+}(\underset{P}{\bar o}^{C'};P)}{[z_M\bar z_M(r_{MZ}r_{MT}-r_{NZ}r_{PT})]^2}\,.
\end{aligned}
\tag{3.51}
$$

Consequently, making contractions over the indices A, B and A', B' yields the expressions (3.22) and (3.27) along with the divergencelessness of

$$\langle L^-(N)R^+(P);\Phi_{AA'}(x)\rangle\,.$$

It should be noted that the densities (3.22), (3.27) and (3.47) differ by an overall sign from those provided by Penrose & Rindler [3]. This is due only to the choice of sign convention involved in the definition of the (variable) inner products at $M^{AA'}$.

There is another property of the configurations shown in Fig. 3 which gives rise to an important alternative expression for the potential density (3.47). The property in question is that the SI quantity $z_M\bar z_M r_{PM}r_{NM}$ remains constant when the relevant integral is performed. A simple way of seeing this is to invoke the formulae (3.12)–(3.15) together with their $(NP\leftrightarrow ZT)$-counterparts. This procedure yields the formal relations

$$\nabla_{AA'}(\log(z_M r_{PM}))=\frac{1}{z_M\bar z_M}\big(\bar z_M\overset{T}{o}_B\nabla_{AA'}\overset{Z}{o}^B+z_M\underset{Z}{\bar o}_{B'}\nabla_{AA'}\underset{T}{\bar o}^{B'}\big)\,,\tag{3.52}$$

$$\nabla_{AA'}(\log(\bar z_M r_{NM}))=\frac{1}{z_M\bar z_M}\big(\bar z_M\overset{T}{o}^B\nabla_{AA'}\overset{Z}{o}_B+z_M\underset{Z}{\bar o}^{B'}\nabla_{AA'}\underset{T}{\bar o}_{B'}\big)\,,\tag{3.53}$$

whence $\nabla_{AA'}(\log(z_M\bar z_M r_{PM}r_{NM}))=0$. Thus, the density (3.47) can be rewritten as

$$
\begin{aligned}
\langle L^-(N)R^+(P);\Phi_{AA'}(x)\rangle &= -\frac{e}{2\pi}\frac{z_N\bar z_P\Delta_0(x;N)\Delta_0(x;P)}{K} \\
&\times\nabla_{AA'}(\log(z_M r_{PM}))\;\underset{N\frac12^-}{\hat\pi}\;\psi_{L^-}(\overset{N}{o}^C;N)\;\underset{P\frac12^+}{\hat\pi}\;\bar\psi_{R^+}(\underset{P}{\bar o}^{C'};P)\,,
\end{aligned}
\tag{3.54}
$$

where K is the scalar quantity defined in (3.11). Similar calculations tell us that the distributional potential density produced by the $\langle R^-(N)L^+(P)\rangle$-current piece (see Eqs (2.37)) can be directly obtained from (3.54) by replacing the $\hat{\pi}$-data and taking a complex conjugation of the remaining factor. Using (3.52) and (3.53), we thus obtain

$$\langle R^-(N)L^+(P);\Phi_{AA'}(x)\rangle = \frac{e}{2\pi}\frac{z_P\bar{z}_N\Delta_0(x;N)\Delta_0(x;P)}{\bar{K}}$$
$$\times\nabla_{AA'}(\log(z_M r_{NM}))\ \underset{N\frac{1}{2}+}{\hat{\pi}}\ \chi_{R-}(\bar{o}_N{}^{C'};N)\ \underset{P\frac{1}{2}-}{\hat{\pi}}\ \bar{\chi}_{L+}({}^{P}o^{C};P). \tag{3.55}$$

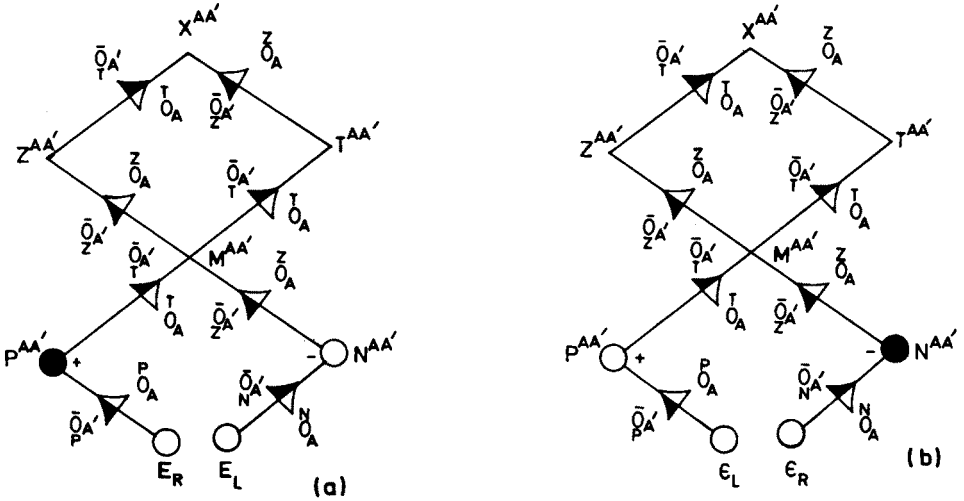

Fig. 10. Minkowskian configurations involved in the explicit integral expressions for the potential densities produced by elementary current pieces. The fact that the integrands carry only the step functions for the points at which the datum spots are centered implies the preservation of the structure of the former calculational devices. The circled loops have the same meaning as before: (a) structure involving a $\psi\bar{\psi}$–current piece; (b) structure involving a $\chi\bar{\chi}$–current piece.

Therefore, the SI expression for the contribution corresponding to this latter density is written as

$$\ll R^-(N)L^+(P);\Phi_{AA'}(x)\gg=$$
$$\int_{\mathcal{E}_{\chi\bar{\chi}}}\langle R^-(N)L^+(P);\Phi_{AA'}(x)\rangle\ \underset{\sim}{\delta}_I\wedge\underset{\sim}{\Omega}^-_N\wedge\underset{\sim}{\delta}_{II}\wedge\underset{\sim}{\Omega}^+_P, \tag{3.56}$$

with the integral being taken over the space of null patterns of the type shown in Fig. 10b. For Eq. (3.56), we have the graphical structure

$$\ll R^{-}(N)L^{+}(P);\phi_{AA'}(x) \gg =$$

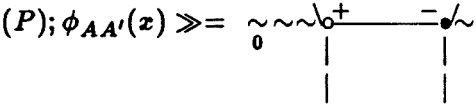

(3.57)

4. Electromagnetic scattering of Dirac fields

We shall now be concerned with evaluating the null configurations that describe the processes of electromagnetic scattering of Dirac fields. The relevant prescriptions are based upon the result that, whenever the structures for the basic potential densities are coupled with the branches corresponding to the KAP-splitting of incoming Dirac fields, all the density equations associated with the former configurations remain formally unaffected. This fact allows one to carry out the actual calculation of the diagrams shown in Figs 5 and 6 systematically. The coupling prescriptions involve modifying the (complex) potential flag poles in such a way that the block carried by the right-hand side of each of the equations governing the propagation of Dirac densities in regions with potential is "annihilated" is case the handedness of the electromagnetic-field branch involved is different from that of the relevant incoming field. Thus, an incoming field of one handedness contributes a spinor to the modified potential kernels which carries the other handedness, but the "strong" statements (3.39), (3.54) and (3.55) still hold, with the formal labels Z and T carried by (3.52) and (3.53) being replaced by R and K, respectively. In the case of Fig. 5, in particular, either of the incoming fields then picks out the piece of the real potential density which involves the electromagnetic datum of the same handedness as that of the associated incoming density. Accordingly, each configuration of Fig. 6 involves a Maxwell-field structure which possesses the same handedness as the corresponding incoming field. The spinor that emanates from the current spot carrying the other handedness thus becomes a "dummy" in the sense that it is taken over by one of the spinors involved in the incoming flag pole. The former spinor is the one whose pole lies on the main plane of the "dual" configuration, the structures of either pair having to be dealt with in this way. In any case, the standard potential kernel is brought back when the incoming Dirac branch is dropped from the relevant structure. For Fig. 6, the main planes of each pair of "dual" configurations turn out to coincide, the NP–ZT interchange rule that emerges from the evaluation of Fig. 3 thus appearing as an NP–RK rule. Indeed, this feature of the IRM-diagrams comes from the wave equations for the Dirac densities exhibited in Section 2.

The explicit expressions for the NID for the scattering processes naturally arise from the solutions of the relevant FDE. We will make use here of the distributional structure of the solutions provided in Ref. [3]. Each such solution carries two pieces which show up as a distributional phase-shift and a scattering term. Both of these terms turn out to vanish when the pertinent incoming field propagates far away from the respective scatterer branch. In this limiting case the incoming field thus propagates as if it were free. All the phase-shift terms involve step functions for the scatterer spots along with Δ_1-functions for the spots from which the incoming fields emanate. These pieces carry also certain scalar functions together with the spinors involved in the KAP-splitting of the incoming fields. The phase-shift scalar functions appear to be constant on $\mathcal{C}_D^+$ and $\mathcal{C}_B^+$ with respect to those derivative operators which are defined in the direction of the propagation of the incoming densities. Such functions play a significant role in the determination of the null data for the processes in that they contribute pieces of elementary data which couple suitably with the structures occurring on the right-hand sides of the interacting FDE, thereby leading to useful (non-vanishing) scattering $\hat{\pi}$-data. Each scattering term involves only the product of a massless free charged spin $\pm\frac{1}{2}$ field density with the step functions for the spotted points of the corresponding configuration. These "electron neutrinos" are effectively required to satisfy certain specific relations set upon the future null cones of the spots involved in the scatterer branches.

The organization of the section is as follows: In subsection 4.1, the calculation of the diagrams of Fig. 5 is carried out. The structures of Fig. 6 are evaluated in subsection 4.2. We will complete the procedures for calculating explicitly just one configuration of each of the figures. The integral expressions for the other configurations will be constructed thereafter on the basis of simple interchange and conjugation rules. Most of the relations involving the derivatives of the spinors and affine parameters carried by the structures under consideration can be obtained from those associated with Fig. 3 by making trivial replacements. For this reason, the entire set of formulae that arise from working out the geometric properties of the scattering diagrams will not be written out explicitly.

4.1. Scattering by $\langle L^0(M); \Phi_{AA'}(x)\rangle$ and $\langle R^0(M); \Phi_{AA'}(x)\rangle$

In order to write down the explicit right-hand sides of the FDE (2.38) and (2.39), we have to replace the complex vector kernels and inner products that enter into the derivative terms of Eq. (3.39) by those for Fig. 5. The corresponding modification of the formulae (3.12)–(3.15) amounts simply to replacing the labels $\langle NZPT\rangle$ by $\langle MKDS\rangle$, respectively. Thus, using the

relations for the latter null structures (see Eq. (3.49))

$$\nabla_{AA'}\left(\overset{K}{o}{}^{L}\nabla_{B}^{A'}\overset{K}{o}{}_{L}\right)=\tfrac{1}{2}\epsilon_{AB}\,\overset{K}{o}{}^{L}\Box\,\overset{K}{o}{}_{L}=0\,, \tag{4.1a}$$

$$\nabla_{AA'}\left(\overset{K}{o}{}^{L}\nabla_{B'}^{A}\overset{K}{o}{}_{L}\right)=\tfrac{1}{2}\epsilon_{A'B'}\,\overset{K}{o}{}^{L}\Box\,\overset{K}{o}{}_{L}=0\,, \tag{4.1b}$$

along with their conjugates, we obtain the density equation

$$\nabla_{AA'}\langle L^{0}(M);\Phi_{B}^{A'}(x)\rangle=\frac{1}{2\pi}\Delta_{1}(x;M)r_{MK}\,\overset{K}{o}{}_{A}\,\bar{\underset{K}{o}}{}_{A'}\left(\overset{K}{o}{}^{L}\nabla_{B}^{A'}\overset{K}{o}{}_{L}\right)\underset{M1^{-}}{\hat{\pi}}\phi_{L^{0}}(\overset{M}{o}{}^{C};M)\,, \tag{4.2}$$

together with the one which involves the right-handed electromagnetic datum. Hence, the expressions for the field densities that emerge from the distributional splitting of the electromagnetic free-field contributions hold on $\mathcal{C}_{M}^{+}$. It must be emphasized that the datum spots producing the incoming Dirac densities do not contribute at all to the integral expressions for the Maxwell quantities which enter into Eqs (2.33). Thus, the Dirac branches of Fig. 5 cease to play any role when the electromagnetic integrals are actually performed. It follows that Eqs (2.38) and (2.39) can be rewritten as

$$\nabla^{AA'}\langle L^{-}(D)L^{0}(M);\psi_{A}(x)\rangle=-\frac{ie}{4\pi^{2}}\frac{z_{m}r_{Dm}\Delta_{0}(x;M)\Delta_{1}(x;D)\,\bar{\underset{S}{o}}{}^{A'}}{\bar{z}_{m}(r_{Dm}r_{MK}+r_{mS}r_{Mm})}$$
$$\times\underset{M1^{-}}{\hat{\pi}}\phi_{L^{0}}(\overset{M}{o}{}^{C};M)\underset{D\frac{1}{2}^{-}}{\hat{\pi}}\psi_{L^{-}}(\overset{D}{o}{}^{L};D)\,, \tag{4.3}$$

$$\nabla^{AA'}\langle R^{-}(D)R^{0}(M);\chi_{A'}(x)\rangle=-\frac{ie}{4\pi^{2}}\frac{\bar{z}_{m}r_{Dm}\Delta_{0}(x;M)\Delta_{1}(x;D)\,\overset{S}{o}{}^{A}}{z_{m}(r_{Dm}r_{MK}+r_{mS}r_{Mm})}$$
$$\times\underset{M1^{+}}{\hat{\pi}}\bar{\phi}_{R^{0}}(\bar{\underset{M}{o}}{}^{C'};M)\underset{D\frac{1}{2}^{+}}{\hat{\pi}}\chi_{R^{-}}(\bar{\underset{D}{o}}{}^{L'};D)\,. \tag{4.4}$$

The standard distributional solution of Eq. (4.3) is given by

$$\langle L^{-}(D)L^{0}(M);\psi_{A}(x)\rangle=\langle L^{-}(D)L^{0}(M);\pi_{A}(x)\rangle\Delta_{0}(x;M)\Delta_{1}(x;D)$$
$$+\langle L^{-}(D)L^{0}(M);S_{A}(x)\rangle\Delta_{0}(x;M)\Delta_{0}(x;D)\,. \tag{4.5}$$

In (4.5), the first term on the right-hand side constitutes the density of phase-shift that occurs due to the presence of a potential density in Eq. (2.38). Its bracketed piece is explicitly written here as the SI expression

$$\langle L^{-}(D)L^{0}(M);\pi_{A}(x)\rangle=U(x)\,\overset{S}{o}{}_{A}\underset{M1^{-}}{\hat{\pi}}\phi_{L^{0}}(\overset{M}{o}{}^{C};M)\underset{D\frac{1}{2}^{-}}{\hat{\pi}}\psi_{L^{-}}(\overset{D}{o}{}^{L};D)\,, \tag{4.6}$$

where $U(x)$ is a well-behaved scalar function of the type $\{0,2;0,0\}$, the relevant scaling acting on the spinor $\overset{K}{o}{}_A$ (see Eq. (4.10) below). The bracketed piece of the second term is a massless free-field density of spin $-1/2$ which actually describes the propagation of the outgoing field. By definition, this latter term satisfies the following relation on $\mathcal{C}_M^+$

$$\langle L^-(D)L^0(M);\mathcal{S}_A(x)\rangle \overset{K}{o}{}^A = 0\,. \tag{4.7}$$

Thus, substituting (4.5) into (4.3) and using SI derivatives of distributions together with (4.7) and the massless-free property

$$\nabla^{AA'}\langle L^-(D)L^0(M);\mathcal{S}_A(x)\rangle = 0\,, \tag{4.8}$$

yields the "reduced" scalar function at $S^{AA'}$

$$\begin{aligned}\langle L^-(D)L^0(M)L^-(S)\rangle &= \langle L^-(D)L^0(M);\mathcal{S}_A(S)\rangle \overset{S}{o}{}^A \\ &= -\frac{ie}{4\pi^2}\frac{z_m \overset{\hat{\pi}}{}_{M1^-}\phi_{L^0}(\overset{M}{o}{}^C;M)\ \overset{\hat{\pi}}{}_{D\frac{1}{2}^-}\psi_{L^-}(\overset{D}{o}{}^L;D)}{\bar{z}_m r_{Mm} r_{DS}}\,,\end{aligned} \tag{4.9}$$

along with the "strong" requirement

$$\begin{aligned}\overset{S}{o}{}_A\nabla^{AA'}U(x) &= -U(x)\frac{r_{Dm}r_{mK}\,\bar{o}_K^{A'}}{\bar{z}_m r_{DS}(r_{Dm}r_{MK}+r_{mS}r_{Mm})} \\ &\quad + \frac{ie}{4\pi^2}\frac{z_m r_{mS}\,\bar{o}_S^{A'}}{\bar{z}_m(r_{Dm}r_{MK}+r_{mS}r_{Mm})}\,.\end{aligned} \tag{4.10}$$

Hence, the function $U(x)$ is constant on $\mathcal{C}_D^+$ with respect to $\partial/\partial r_{DS} = \overset{S}{o}{}^A\bar{o}_S^{A'}\nabla_{AA'}$ whence a suitable displacement of the "reduced" form of Fig. 5a leads us to

$$\frac{\partial}{\partial r_{DS}}U(x) = 0\,. \tag{4.11}$$

It is of some interest to re-define the phase-shift function as $U(x) = \frac{W(x)}{z_m r_{Mm}}$, with $W(x)$ satisfying (4.11). In this connection, we should notice that the quantity $z_m r_{Mm}$ is also constant along generators of $\mathcal{C}_D^+$. In fact,

the latter form exhibits the desirable behaviour of (4.6). The phase-shift integral is, therefore, written as

$$\ll L^-(D)L^0(M);\pi_A(x)\gg=\int_{\mathcal{P}_L}\langle L^-(D)L^0(M);\pi_A(x)\rangle\Delta_0(x;M)\Delta_1(x;D)\times\underset{\sim}{\Omega}{}^0_M\wedge\underset{\sim}{\omega}_I\wedge\underset{\sim}{\Omega}{}^-_D\,,\qquad(4.12)$$

which is taken over the space $\mathcal{P}_L$ of null patterns of the type shown in Fig. 11a, the ω-form being involved in the formation of $D^{AA'}$. Its graphical representation is depicted as

$\ll L^-(D)L^0(M);\pi_A(x)\gg=$ 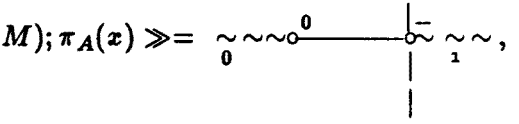 , (4.13)

with the internal line thus denoting the whole U-function.

The scalar function (4.9) is indeed the $\{1,0;0,0\}$-null datum at $S^{AA'}$ for the scattering process controlled by Eq. (2.38). Now, using the $\hat{\pi}$-operator

$$\underset{S\frac{1}{2}^-}{\hat{\pi}}=\frac{r_{DS}}{z_S}\Big\{\mathbb{D}(S;\gamma_S)+\frac{2}{r_{DS}}\Big\}\,,\qquad(4.14)$$

and setting $z_S=\overset{S}{o}{}^A\overset{X}{o}{}_A$, we obtain the $\{0,-1;0,0\}$-datum for the process

$$\ll L^-(D)L^0(M)L^-(S)\gg=-\frac{ie}{4\pi^2}\frac{z_m\underset{M1^-}{\hat{\pi}}\phi_{L^0}(\overset{M}{o}{}^C;M)\underset{D\frac{1}{2}^-}{\hat{\pi}}\psi_{L^-}(\overset{D}{o}{}^L;D)}{\bar{z}_m z_S r_{Mm} r_{DS}}\,.\qquad(4.15)$$

In consequence, the relevant scattering integral becomes

$$\ll L^-(D)L^0(M)L^-(S);S_A(x)\gg=\int_{\Sigma_L}\overset{X}{o}{}_A\ll L^-(D)L^0(M)L^-(S)\gg\Delta_0(x;M)\Delta_0(x;D)\times\underset{\sim}{\Omega}{}^0_M\wedge\underset{\sim}{\omega}_I\wedge\underset{\sim}{\Omega}{}^-_D\wedge\mathcal{K}^-_S\,,\qquad(4.16)$$

with $\mathcal{K}^-_S$ being the KAP-form at $S^{AA'}$, and the space Σ_L of null structures over which the integration is to be performed consisting of configurations of

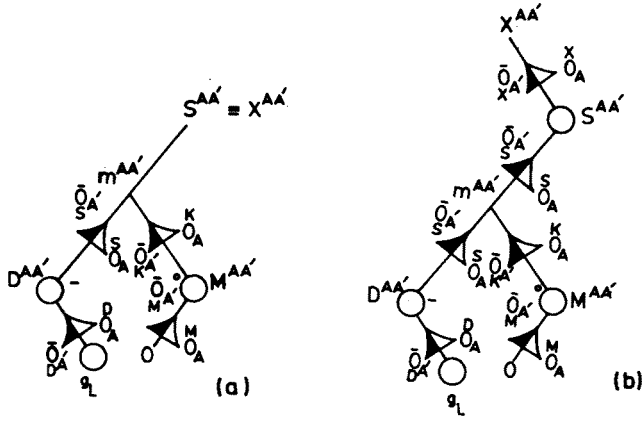

Fig. 11. Null patterns involved in the evaluation of the elementary contribution arising from the interaction between an incoming left-handed Dirac density and the real potential density. The loop denotes the IRM-structure occurring in the formation of the Dirac spot that produces the incoming field. The relevant branches of the underlying calculational device have been displaced suitably: (a) phase-shift; (b) scattering.

the type exhibited in Fig. 11b. Graphically for Eq. (4.16), we have

$$\ll L^-(D)L^0(M)L^-(S);S_A(x)\gg=$$

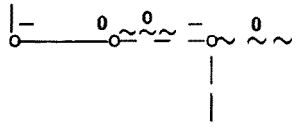

(4.17)

where the internal solid line represents the overall inner-product affine-parameter block occurring in (4.15).

The contributions associated with the distributional solution of Eq. (2.39) can be readily constructed from those obtained above by first replacing the $\hat{\pi}$-data, and then taking a complex conjugation of the inner products carried explicitly by (4.15). This result amounts to changing the color of the vertices borne by the graphs (4.13) and (4.17). Thus the corresponding phase-shift expression is depicted as

$$\ll R^-(D)R^0(M);\Pi_{A'}(x)\gg=$$

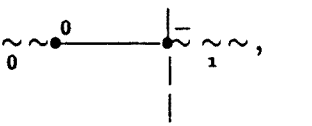

(4.18)

and the scattering integral as

$$\ll R^{-}(D)R^{0}(M)R^{-}(S);S_{A'}(x)\gg=$$

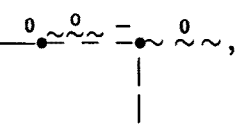

(4.19)

with the (scattering) $\hat{\pi}$-datum involved in the latter structure being

$$\ll R^{-}(D)R^{0}(M)R^{-}(S)\gg= \\ -\frac{ie}{4\pi^2}\frac{\bar{z}_m \underset{M1+}{\hat{\pi}}\,\bar{\phi}_{R^0}(\bar{o}_M^{\,C'};M)\,\underset{D\frac{1}{2}+}{\hat{\pi}}\,\chi_{R^-}(\bar{o}_D^{\,L'};D)}{z_m\bar{z}_{S^r}M_{m^r}D_S}. \tag{4.20}$$

The configurations for the integrals represented by (4.18) and (4.19) are shown in Fig. 12.

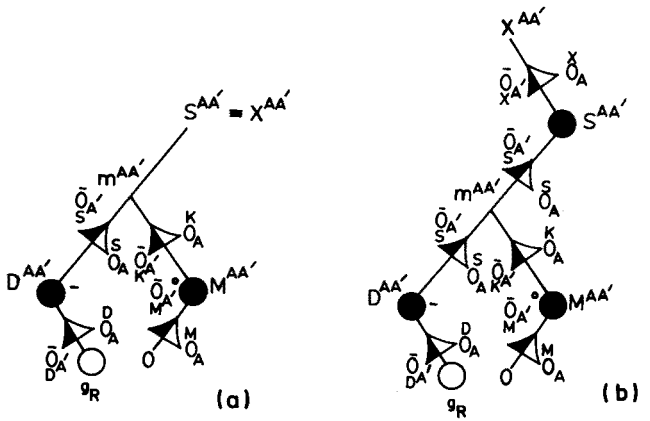

Fig. 12. Null patterns involved in the evaluation of the elementary contribution arising from the interaction between an incoming right-handed Dirac density and the "zeroth-order" potential density. The loop denotes the underlying configuration which gives rise to the formation of the Dirac spot producing the incoming field. The relevant branches have been suitably displaced: (a) phase-shift; (b) scattering.

4.2. Scattering by higher-order elementary potentials

We have seen that the colored graphs which represent the scattering terms coming from the evaluation of Fig. 5 do not involve any splitting of the data for the processes. This feature is related to the fact that each of the scatterer structures partaking of the processes carries only a single

spotted vertex. Thus, as the situation stands, the graphs do not carry any specific information concerning the individual pieces of the relevant data. We shall now see that the graphs associated with the scattering pieces of the elementary contributions arising from the calculation of Fig. 6 bring out naturally such a splitting of the data. In accordance with this latter fact, internal solid lines that join vertices corresponding to current spots appear as contributions due to scatterer branches whilst contributions due to incoming branches are represented by internal solid lines that connect current blocks and KAP-vertices. The pattern of the explicit distributional statements coming into play here is the same as that of the structures used in the previous subsection, but each piece of the solutions of the FDE now involves three distributions.

Only the calculation of the IRM-structure associated with Eq. (2.42) will be explicitly carried out, but it is convenient to introduce also the inner products for the configurations associated with Eqs (2.43)–(2.45). We have, in effect,

$$z_N = {}^{N}_{O}{}^{A}\,{}^{R}_{O}{}_{A},\ z_P = {}^{P}_{O}{}^{A}\,{}^{K}_{O}{}_{A},\ z_m = {}^{R}_{O}{}^{A}\,{}^{K}_{O}{}_{A}, \tag{4.21a}$$

$$z_D = {}^{D}_{O}{}^{A}\,{}^{\sigma}_{O}{}_{A},\ z_F = {}^{R}_{O}{}^{A}\,{}^{\sigma}_{O}{}_{A},\ z_B = {}^{B}_{O}{}^{A}\,{}^{\Sigma}_{O}{}_{A},\ z_G = {}^{K}_{O}{}^{A}\,{}^{\Sigma}_{O}{}_{A}, \tag{4.21b}$$

along with their conjugates. At this stage, all the procedures rest crucially upon the fact that statements of the type (4.1) involving the basis spinors of Fig. 6 are also true. The relevant K-scalar is readily obtained from that for Fig. 3 by replacing the labels Z and T by R and K, respectively, but the SI real vector $\alpha^{AA'} = r_{NF}\,{}^{R}_{O}{}^{A}\,\bar{o}_{R}{}^{A'} - r_{DF}\,{}^{\sigma}_{O}{}^{A}\,\bar{o}_{\sigma}{}^{A'}$ is also held fixed as $x^{AA'}$ varies in a suitable way. For the relations defining the position of $x^{AA'}$, we have

$$x^{AA'} = N^{AA'} + r_{NR}\,{}^{R}_{O}{}^{A}\,\bar{o}_{R}{}^{A'} + r_{RX}\,{}^{\sigma}_{O}{}^{A}\,\bar{o}_{\sigma}{}^{A'}, \tag{4.22a}$$

$$x^{AA'} = P^{AA'} + r_{Pm}\,{}^{K}_{O}{}^{A}\,\bar{o}_{K}{}^{A'} + r_{mR}\,{}^{R}_{O}{}^{A}\,\bar{o}_{R}{}^{A'} + r_{RX}\,{}^{\sigma}_{O}{}^{A}\,\bar{o}_{\sigma}{}^{A'}, \tag{4.22b}$$

$$x^{AA'} = D^{AA'} + r_{D\sigma}\,{}^{\sigma}_{O}{}^{A}\,\bar{o}_{\sigma}{}^{A'} + r_{\sigma X}\,{}^{R}_{O}{}^{A}\,\bar{o}_{R}{}^{A'}. \tag{4.22c}$$

Thus, differentiating out (4.22) and making appropriate contractions we derive the relations

$$\nabla_{AA'}\,{}^{K}_{O}{}^{B} = -\frac{z_m r_{Nm} r_{DF}}{\bar{z}_m z_P z_F r_{Pm}(r_{NF}r_{D\sigma} + r_{FR}r_{DF})}\,{}^{\sigma}_{O}{}^{A}\,\bar{o}_{R}{}^{A'}\,{}^{P}_{O}{}^{B}, \tag{4.23}$$

$$\nabla_{AA'} r_{Pm} = \left(\frac{r_{Nm}r_{DF}}{z_m\bar{z}_m}\right)\left[\frac{z_P z_F \bar{z}_m(\bar{o}_{R}{}^{B'}\,\bar{o}_{P}{}_{B'})\,{}^{R}_{O}{}^{A}\,\bar{o}_{\sigma}{}^{A'} + \text{c.c.}}{z_P z_F \bar{z}_P \bar{z}_F(r_{NF}r_{D\sigma} + r_{FR}r_{DF})}\right], \tag{4.24}$$

$$\nabla_{AA'} r_{Nm} = \left(\frac{r_{Nm} r_{DF}}{z_m \bar{z}_m}\right)\left[\frac{z_N z_m \bar{z}_F (\underset{K}{\bar{o}}{}^{B'} \underset{N}{\bar{o}}{}_{B'}) \overset{\sigma}{o}{}_A \underset{R}{\bar{o}}{}_{A'} + \text{c.c.}}{z_N z_F \bar{z}_N \bar{z}_F (r_{NF} r_{D\sigma} + r_{FR} r_{DF})}\right] , \quad (4.25)$$

together with the conjugate of (4.23) and those expressions which are derived from (3.12)–(3.15) by making the simultaneous replacements $\langle NZMPT\rangle \leftrightarrow \langle NRFD\sigma\rangle$. It should be pointed out that, as regards Eqs (4.24) and (4.25), the $NP - RK$ interchange rule applies only to the spin inner products. This is because the standard flag poles $\{\overset{R}{o}{}^A \underset{K}{\bar{o}}{}^{A'}, \overset{K}{o}{}^A \underset{R}{\bar{o}}{}^{A'}\}$ actually enter into the picture only when the null patterns of either pair of "dual" configurations are appropriately combined together.

To write out the explicit right-hand side of Eq. (2.42), one has first to re-instate the expression (3.22) by adapting the pattern of either of the potential densities (3.47) and (3.54) to the situation depicted in Fig. 6a. This task can be easily carried out by taking the derivative of the SI vector associated with the K-scalar for the configuration being considered as well as suitably contracted second derivatives of $\overset{R}{o}{}^A$ and $\underset{K}{\bar{o}}{}^{A'}$. Thus, making use of the derivative relations arising from (4.22), after some calculations we obtain the statements

$$\frac{z_m}{\bar{z}_m}(\nabla_{AA'} \underset{R}{\bar{o}}{}_{M'})\nabla_B^{A'} \underset{K}{\bar{o}}{}^{M'} + (\nabla_{AA'} \overset{K}{o}{}_M)\nabla_B^{A'} \overset{R}{o}{}^M - \frac{z_m}{\bar{z}_m^2}(\underset{R}{\bar{o}}{}_{M'} \nabla_B^{A'} \underset{K}{\bar{o}}{}^{M'})$$
$$\times \underset{K}{\bar{o}}{}_{T'} \nabla_{AA'} \underset{R}{\bar{o}}{}^{T'} + \frac{1}{z_m}(\overset{K}{o}{}_M \nabla_B^{A'} \overset{R}{o}{}^M) \overset{R}{o}{}_T \nabla_{AA'} \overset{K}{o}{}^T = 0 , \quad (4.26)$$

$$\overset{K}{o}{}_M \nabla_{A'[A} \nabla_{B]}^{A'} \overset{R}{o}{}^M = 0 = \tfrac{1}{2}\varepsilon_{AB} \overset{K}{o}{}_M \Box \overset{R}{o}{}^M , \quad (4.27)$$

and

$$\underset{R}{\bar{o}}{}_{M'} \nabla_{A'[A} \nabla_{B]}^{A'} \underset{K}{\bar{o}}{}^{M'} = 0 = \tfrac{1}{2}\varepsilon_{AB} \underset{R}{\bar{o}}{}_{M'} \Box \underset{K}{\bar{o}}{}^{M'} . \quad (4.28)$$

Hence, invoking the modified RK-version of (3.52), we get the equations

$$\nabla_{A'[A} \nabla_{B]}^{A'} (\log(z_m r_{Pm})) = 0 \leftrightarrow \Box(\log(z_m r_{Pm})) = 0 , \quad (4.29)$$

which, when combined with $\nabla_{AA'} \Delta_0(x;P) = 0$ on C_N^+ yield the SI statement

$$\nabla_{AA'} \langle L^-(N) R^+(P); \Phi_B^{A'}(x)\rangle = \frac{-e}{2\pi} \overset{R}{o}{}_A \overset{R}{o}{}_B \frac{\Delta_1(x;N)\Delta_0(x;P)}{z_m r_{Pm}}$$
$$\times \underset{N\frac{1}{2}^-}{\hat{\pi}} \psi_{L^-}(\overset{N}{o}{}^C; N) \underset{P\frac{1}{2}^+}{\hat{\pi}} \bar{\psi}_{R^+}(\underset{P}{\bar{o}}{}^{L'}; P) . \quad (4.30)$$

We have, therefore, been led to the "reduced" version of Eq. (3.42). It turns out that Eq. (2.42) takes the explicit form

$$\nabla^{AA'}\langle L^-(D)R^+(P)L^-(N);\psi_A(x)\rangle =$$
$$-\frac{ie^2}{4\pi^2}\frac{z_F r_{DF}\Delta_0(x;N)\Delta_0(x;P)\Delta_1(x;D)\,\bar{o}_\sigma^{\,A'}}{z_m\bar{z}_F r_{Pm}(r_{NF}r_{D\sigma}+r_{FR}r_{DF})}$$
$$\times \hat{\pi}_{N\frac{1}{2}^-}\psi_{L^-}({}^N_o C;N)\,\hat{\pi}_{P\frac{1}{2}^+}\bar{\psi}_{R^+}(\bar{o}_P^{\,L'};P)\,\hat{\pi}_{D\frac{1}{2}^-}\psi_{L^-}({}^D_o C;D). \quad (4.31)$$

Now, inserting into (4.31) the expression

$$\langle L^-(D)R^+(P)L^-(N);\psi_A(x)\rangle =$$
$$\langle L^-(D)R^+(P)L^-(N);\mathcal{P}_A(x)\rangle\Delta_0(x;N)\Delta_0(x;P)\Delta_1(x;D)$$
$$+\langle L^-(D)R^+(P)L^-(N);\Sigma_A(x)\rangle\Delta_0(x;N)\Delta_0(x;P)\Delta_0(x;D), \quad (4.32)$$

along with the defining relations

$$\nabla^{AA'}\langle L^-(D)R^+(P)L^-(N);\Sigma_A(x)\rangle = 0, \quad (4.33a)$$
$$\langle L^-(D)R^+(P)L^-(N);\Sigma_A(x)\rangle\,{}^R_o{}^A = 0, \quad (4.33b)$$
$$\langle L^-(D)R^+(P)L^-(N);\Sigma_A(x)\rangle\,{}^K_o{}^A = 0, \quad (4.33c)$$

and invoking once again the generalized pattern of derivatives of distributions, we require the following SI expression

$$\nabla^{AA'}\langle L^-(D)R^+(P)L^-(N);\mathcal{P}_A(x)\rangle - \langle L^-(D)R^+(P)L^-(N);\mathcal{P}_A(x)\rangle$$
$$\times\frac{{}^R_o{}^A\,\bar{{}^R_o}^{A'}}{z_F\bar{z}_F r_{D\sigma}} + \langle L^-(D)R^+(P)L^-(N);\Sigma_A(x)\rangle r_{D\sigma}\,{}^\sigma_o{}^A\,\bar{o}_\sigma^{\,A'}$$
$$= -\frac{ie^2}{4\pi^2}\frac{z_F r_{DF}\,\bar{o}_\sigma^{\,A'}}{z_m\bar{z}_F r_{Pm}(r_{NF}r_{D\sigma}+r_{FR}r_{DF})}$$
$$\times\hat{\pi}_{N\frac{1}{2}^-}\psi_{L^-}({}^N_o C;N)\,\hat{\pi}_{P\frac{1}{2}^+}\bar{\psi}_{R^+}(\bar{o}_P^{\,L'};P)\,\hat{\pi}_{D\frac{1}{2}^-}\psi_{L^-}({}^D_o C;D). \quad (4.34)$$

Strictly speaking, the distributional statement associated with Eq. (4.34) holds on $\mathcal{C}_D^+$ whence the expression involved in the general situation actually carries the "reduced" form of the denominator of the piece that bears the coupling constant. It follows that, writing

$$\langle L^-(D)R^+(P)L^-(N);\mathcal{P}_A(x)\rangle = \frac{V(x)}{z_m r_{Pm}r_{NF}}\,{}^\sigma_o{}_A\,\hat{\pi}_{N\frac{1}{2}^-}\psi_{L^-}({}^N_o C;N)$$
$$\times\hat{\pi}_{P\frac{1}{2}^+}\bar{\psi}_{R^+}(\bar{o}_P^{\,L'};P)\,\hat{\pi}_{D\frac{1}{2}^-}\psi_{L^-}({}^D_o C;D), \quad (4.35)$$

we obtain the following expression at $\sigma^{AA'}$

$$\langle L^-(D)R^+(P)L^-(N)L^-(\sigma)\rangle = \langle L^-(D)R^+(P)L^-(N);\Sigma_A(\sigma)\rangle \overset{\sigma}{o}{}^A$$
$$= -\frac{ie^2}{4\pi^2}\frac{z_F}{z_m\bar{z}_F r_{Pm}r_{NF}r_{D\sigma}}\hat{\pi}_{N\frac{1}{2}^-}\psi_{L^-}(\overset{N}{o}{}^C;N)$$
$$\times \hat{\pi}_{P\frac{1}{2}^+}\bar{\psi}_{R^+}(\bar{o}_P{}^{L'};P)\hat{\pi}_{D\frac{1}{2}^-}\psi_{L^-}(\overset{D}{o}{}^C;D), \tag{4.36}$$

provided that

$$\overset{\sigma}{o}{}_A\nabla^{AA'}W(x) = W(x)\frac{r_{FR}r_{DF}\,\bar{o}_R{}^{A'}}{\bar{z}_F r_{D\sigma}(r_{NF}r_{D\sigma}+r_{FR}r_{DF})}$$
$$+\frac{ie^2}{4\pi^2}\frac{z_F r_{F\sigma}\,\bar{o}_\sigma{}^{A'}}{z_m\bar{z}_F r_{Pm}(r_{NF}r_{D\sigma}+r_{FR}r_{DF})}, \tag{4.37}$$

with $W(x) = \frac{V(x)}{z_m r_{Pm}r_{NF}}$. Equation (4.35) defines the explicit SI kernel of the phase-shift density for the configuration under consideration. The scalar function $W(x)$ can carry only spin weights for $\overset{R}{o}{}^A$ and $\bar{o}_K{}^{A'}$ as a quantity of the type $\{1,0;1,0\}$. It clearly satisfies $\partial/\partial r_{D\sigma}W(x)=0$ on $\mathcal{C}_D^+$, and, therefore, so does $V(x)$, since $\partial/\partial r_{D\sigma}\left(\frac{1}{z_m r_{Pm}r_{NF}}\right)=0$. Thus, the phase-shift integral is written as

$$\ll L^-(D)R^+(P)L^-(N);\mathcal{P}_A(x)\gg = \int_{\pi_L}\langle L^-(D)R^+(P)L^-(N);\mathcal{P}_A(x)\rangle$$
$$\times \Delta_0(x;N)\Delta_0(x;P)\Delta_1(x;D)\,\underset{\sim}{\vartheta}_I\wedge\underset{\sim}{\Omega}{}^-_N\wedge\underset{\sim}{\vartheta}_{II}\wedge\underset{\sim}{\Omega}{}^+_P\wedge\underset{\sim}{\vartheta}_{III}\wedge\underset{\sim}{\Omega}{}^-_D, \tag{4.38}$$

where π_L denotes the space of null configurations of the type depicted in Fig. 13a, and the ϑ-forms bear the same meaning as before. For the corresponding graph, we have

$\ll L^-(D)R^+(P)L^-(N);\mathcal{P}_A(x)\gg =$ 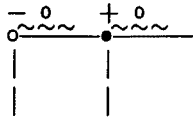 . (4.39)

For convenience, the internal solid line that connects the vertices associated with the current spots has been arbitrarily taken to represent the quantity

$\frac{1}{z_m r_{Pm} r_{NF}}$. The reason for this convention is the fact that it may eventually be useful to ascribe a standard internal structure to the current branches of Fig. 6. The function $V(x)$ is represented by the line which connects the blocks associated with the incoming field and scatterer. When the incoming Dirac branch is disconnected from the structure, the contribution involving r_{NF} "evaporates", and the step function $\Delta_0(x;N)$ gets replaced by $\Delta_1(x;N)$. We can easily see that the first term on right-hand side of (4.37) actually cancels that coming from the combination of the derivatives of $\overset{\sigma}{o}{}^A$ and $\Delta_1(x;D)$. The second piece couples together with the right-hand side of Eq. (4.31), thus yielding the appropriate null-datum expression. It now becomes clear that if the former potential flag pole had been utilized for calculating the scattering diagram, the information about the null datum for the process would have been lost since the spinors $\overset{R}{o}{}^A$, $\overset{K}{o}{}^A$ and $\overset{\sigma}{o}{}^A$ and their conjugates are taken to be independent. Obviously, similar considerations are also applicable to the case of Eqs (4.3) and (4.4).

In fact, (4.36) is the expression for the $\{1,0;0,0\}$-datum for the process. Hence, setting $z_\sigma = \overset{\sigma}{o}{}^A \overset{X}{o}{}_A$, we obtain the following expression for the corresponding $\hat{\pi}$-datum

$$\ll L^-(D)R^+(P)L^-(N)L^-(\sigma) \gg = -\frac{ie^2}{4\pi^2} \frac{z_F}{z_m \bar{z}_F z_\sigma r_{Pm} r_{NF} r_{D\sigma}}$$
$$\times \underset{N\frac{1}{2}^-}{\hat{\pi}} \psi_{L^-}(\overset{N}{o}{}^C; N) \underset{P\frac{1}{2}^+}{\hat{\pi}} \bar{\psi}_{R^+}(\bar{\overset{}{o}}{}^{L'}_P; P) \underset{D\frac{1}{2}^-}{\hat{\pi}} \psi_{L^-}(\overset{D}{o}{}^C; D), \qquad (4.40)$$

whence the relevant scattering integral turns out to be given by

$$\ll L^-(D)R^+(P)L^-(N)L^-(\sigma); \Sigma_A(x) \gg =$$
$$\int_{\mathcal{X}_L} \overset{X}{o}{}_A \ll L^-(D)R^+(P)L^-(N)L^-(\sigma) \gg \Delta_0(x;N)\Delta_0(x;P)\Delta_0(x;D)$$
$$\times \underset{\sim}{\mathcal{N}}{}^-_N \wedge \underset{\sim}{\mathcal{N}}{}^+_P \wedge \underset{\sim}{\mathcal{N}}{}^-_D \wedge \underset{\sim}{\mathcal{K}}{}^-_\sigma, \qquad (4.41)$$

where $\underset{\sim}{\mathcal{N}}{}^-_V$ denotes $\underset{\sim}{\vartheta}_{\mathcal{A}} \wedge \underset{\sim}{\Omega}{}^-_V$, with the letter V (resp. $\mathcal{A}$) standing for either N, P or D (resp. I, II or III). The integral (4.41) is taken over the space $\mathcal{X}_L$ of the configurations shown in Fig. 13b. Its associated graph is depicted as

$$\ll L^-(D)R^+(P)L^-(N)L^-(\sigma); \Sigma_A(x) \gg =$$

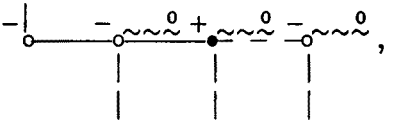

(4.42)

with the internal solid line that connects the "wavy-line-free" vertex denoting the datum piece $z_F/\bar{z}_F z_\sigma \tau_{D\sigma}$. We stress that a structure without a distribution for $D^{AA'}$ also arises here, when we perform the potential integral which involves the (common) solution of Eqs (3.42) and (3.43). Thus, the incoming Dirac densities appear to be meaningful only when the scattering processes are explicitly considered.

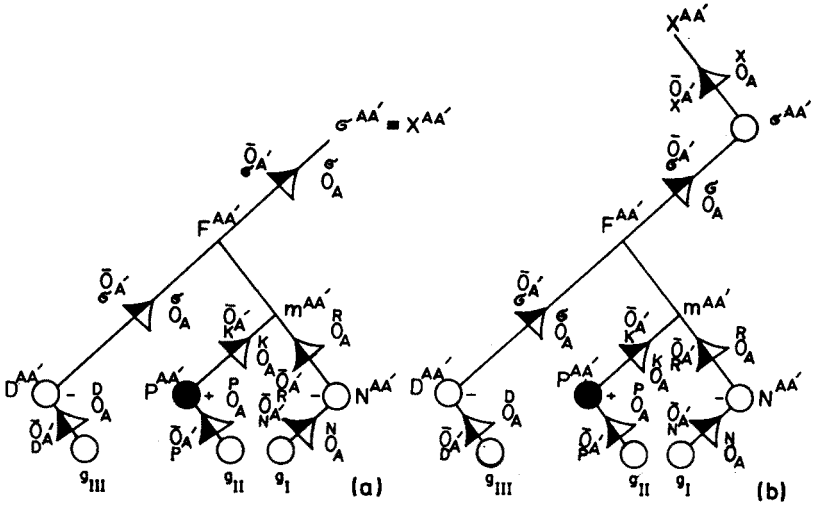

Fig. 13. Null graphs associated with the integrations involving the distributional solution of Eq. (2.42). The loops denote the structures involved in the formation of the datum spots occurring in Fig. 6a. The end vertices have been taken to coincide with $x^{AA'}$: (a) phase-shift; (b) scattering.

The prescriptions for evaluating the other configurations of Fig. 6 are essentially the same as those worked out before. All the quantities entering into the integrals for Fig. 6b can be immediately obtained from those for Fig. 6a by first applying the simultaneous interchanges $\sigma \leftrightarrow \Sigma$, $F \leftrightarrow G$, $D \leftrightarrow B$ $N \leftrightarrow P$, along with a complex conjugation, and then replacing the $\hat{\pi}$-datum that generates the incoming density. This constitutes the interchange rule which enables us to write down the field integral for one configuration on the basis of that for the corresponding "dual" structure. Roughly speaking, the integrals for Fig. 6c can be constructed from (4.38) and (4.41) by replacing z_F, z_m and z_σ by their conjugates and the ψ-data by χ-data. At this point, one might set up at once the formulae for Fig. 6d by using the interchange rule given above. We should observe that this rule actually arises out of replacing the conjugate potential kernels $\overset{R}{o}{}_A \bar{o}_{\sigma A'}$, $\overset{\sigma}{o}{}_A \bar{o}_{R A'}$, by $\overset{\Sigma}{o}{}_A \bar{o}_{K A'}$, $\overset{K}{o}{}_A \bar{o}_{\Sigma A'}$, respectively. For the scattering process of

Fig. 6b, for instance, we thus obtain the $\hat{\pi}$-datum (see Eq. (2.43))

$$\ll R^-(B)L^-(N)R^+(P)R^-(\Sigma) \gg = -\frac{ie^2}{4\pi^2} \frac{\bar{z}_G}{\bar{z}_m z_G \bar{z}_\Sigma r_{Nm} r_{PG} r_{B\Sigma}}$$
$$\times \underset{N\frac{1}{2}^-}{\hat{\pi}} \psi_{L^-}(\overset{N}{o}{}^C; N) \underset{P\frac{1}{2}^+}{\hat{\pi}} \bar{\psi}_{R^+}(\bar{o}_P{}^{L'}; P) \underset{B\frac{1}{2}^+}{\hat{\pi}} \chi_{R^-}(\bar{o}_B{}^{C'}; B). \qquad (4.43)$$

Accordingly, we have the graphical representation displayed in Table I.

TABLE I

Symbolic expressions and colored graphs for the configurations b, c and d of Fig. 6.

PHASE-SHIFT

	GRAPHS
$\ll R^-(B)L^-(N)R^+(P); P_{A'}(x) \gg$	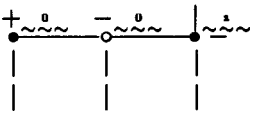
$\ll R^-(D)L^+(P)R^-(N); \mathcal{P}_{A'}(x) \gg$	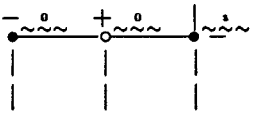
$\ll L^-(B)R^-(N)L^+(P); \mathrm{P}_A(x) \gg$	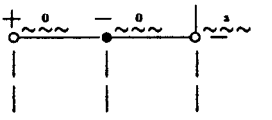

SCATTERING

	GRAPHS
$\ll R^-(B)L^-(N)R^+(P)R^-(\Sigma); \sigma_{A'}(x) \gg$	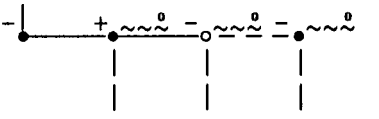
$\ll R^-(D)L^+(P)R^-(N)R^-(\sigma); s_{A'}(x) \gg$	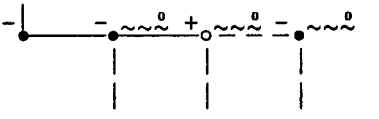
$\ll L^-(B)R^-(N)L^+(P)L^-(\Sigma); S_A(x) \gg$	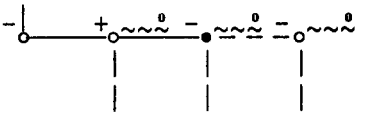

5. Concluding remarks and outlook

One remarkable feature of the IRM-expressions presented here, which has also arisen as a consequence of the particular choice of NID for all the distributional contributions, is related to the simplicity of the form of the potential and field integrals. The introduction of null data for potentials on $\mathcal{C}_0^+$ would entail the generation of additional electromagnetic fields which would, in turn, produce further elementary Dirac current pieces. The procedure for working out the corresponding FDE would therefore be reversed, but the new integral expressions would not provide any further insight into the whole picture. It was seen that the procedure involving a suitable modification of the potential vector kernels gives rise automatically to adequate NID expressions for the processes. However, we should point out that such a procedure does not yield any explicit expressions for the scattering densities. The requirements amounting to the vanishing of the scattering data on the future null cones of the spotted vertices that occur in the scatterer branches, were indeed made in order to balance the "degrees" of the distributions involved in the interacting FDE. An important feature of these data is the fact that the datum contributions due to incoming densities are naturally separable from those due to scatterers. It is believed that this property can eventually play a significant role in a quantum description of the scattering processes. In this connection, it would be convenient to employ the usual definition of the charge-helicity conjugation which actually preserves the handedness of the Dirac fields. The helicity of the electromagnetic-field subgraphs occurring in the scattering diagrams would, consequently, be specified by the sign of the charge borne by appropriate current spots. Nevertheless, both the masslessness of the Maxwell fields and the divergencelessness of the potentials must be retained, regardless of whether the conjugate Dirac fields are effectively taken to propagate towards the past.

Of course, the structure of the statements involving the directional derivatives of the phase-shift functions leads immediately to expressions which allow one to calculate explicitly any phase-shift integral. The constants arising from the integration of the relevant differential equations have to be specified so as to avoid the vanishing of the densities on the future null cones of the spots that generate the incoming fields. In the case of (4.10), for example, the integration constant appears to be proportional to $1/r_{mK}$. When the contractions yielding the directional derivative relations are made, the pieces of the defining expressions that contribute to the scattering data are "annihilated". Hence the role played by these datum pieces is to make up the data, thereby "neutralizing" the vanishing of the $\hat{\pi}$-expressions which arise from the combination of the contributions due to derivatives of $\Delta_0(x; D)$ and $\Delta_0(x; B)$ with the right-hand sides of the Dirac FDE.

It is worth remarking that the graphs which enter into the standard mass-scattering expressions recovering the Dirac fields [7, 10] can also be associated with colored trees of the type defined in subsection 2.4. Thus, the only internal lines carried by these trees appear to be solid lines. The structure associated which each such line consists of a single affine parameter while each of the colored vertices turns out to represent also an inner product. The parameter is the one which connects the spots associated with the vertices joined by the lines. Such spots always carry spinors bearing opposite helicities whence each internal line now connects two vertices carrying different colors. Any one of the inner products is set up at the IRM-point which corresponds to the vertex associated with it, whence the middle vertex occurring in any two-adjacent-edge branch contributes just one inner product to a massive integrand. Their specification is attained by using a trivial white-black rule. For a field of order N, the tree thus possesses N colored vertices carrying wavy lines together with one vertex which actually bears the (external) spinor line. All the wavy lines carry the number 0. In the left-handed case, the vertex associated with the datum spot lying on $\mathcal{C}_0^+$ is taken to be white or black if N is even or odd, respectively. For an even-order (resp. odd-order) field, the graph accordingly carries $\frac{N}{2}+1$ $\left(\text{(resp. } \frac{N+1}{2}\right)$ white vertices and $\frac{N}{2}$ $\left(\text{resp. } \frac{N+1}{2}\right)$ black vertices. For the right-handed contribution of the same order, the colored-vertex configuration is evidently similar to the previous one, but the other way round. Hence, the number of internal lines occurring in any graph equals the order of the corresponding field in the case of either handedness. The expression for the entire left-handed field, for instance, turns out then to be given by

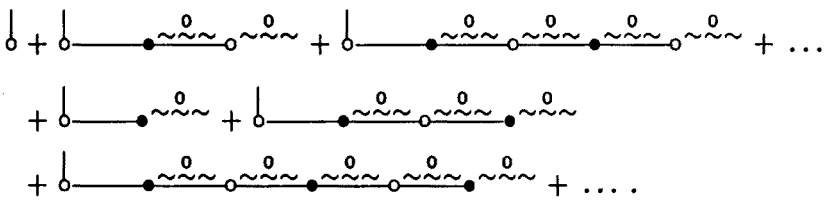

It becomes clear that our graphical label device can be particularly utilized for calculating potential-field contributions which involve the coupling of several basic null configurations.

It is of some importance to observe that the phase-shift and electromagnetic-field integral expressions take a considerably simpler form whenever we make use of statements of the type

$$\int_{\mathcal{G}} f(x)\Delta_1(x;M)\,\underset{\sim}{\Omega}_M = \int_{\mathcal{G}} f(0)\,\underset{\sim}{\mathcal{K}}_M\,.$$

This procedure entails removing the wavy line from the (colored) vertex corresponding to $M^{AA'}$, and restricts the values of some appropriate function $f(x)$ to those specified on $\mathcal{C}_M^+$ for which $x^{AA'}x_{AA'} = 0$. It turns out that vertices carrying external dashed lines without wavy lines have ultimately to be taken into consideration.

The important question concerning the convergence of the graphical expansions which recover the entire set (2.1) still constitutes an open problem. We think that the use of an appropriate twistor version of the IRM-patterns exhibited in Sections 3 and 4 would shed some light on this situation. The crucial point here is, in effect, that the evaluation of the twistorial integrals for typical distributional contributions might lead to explicit expansions possessing very simple properties. In the absence of electromagnetism, this insight would be particularly brought about by employing the transcription techniques provided by Cardoso [16] in connection with the construction of a twistorial representation of the mass-scattering integrals. Further investigation along these lines will probably be carried out elsewhere.

I wish to acknowledge Dr Asghar Qadir for making some invaluable suggestions. My warmest thanks go to the World Laboratory for financial support.

REFERENCES

[1] R. Penrose, *Conformal Approach to Infinity*, in *Relativity, Groups and Topology*, The 1963 Les Houches Lectures, ed. B.S. DeWitt and C.M. DeWitt, Gordon and Breach, New York 1964.
[2] R. Penrose, *Gen. Relativ. Gravitation* **12**, 225 (1980).
[3] R. Penrose, W. Rindler, *Spinors and Space-Time*, Vol. 1, CUP, Cambridge 1984.
[4] J.G. Cardoso, *Int. J. Theor. Phys.* **4**, 447 (1991).
[5] J.G. Cardoso, *J. Math. Phys.* **33**, 1 (1992).
[6] J.G. Cardoso, M. Sci. Thesis, University of Oxford, 1988.
[7] J.G. Cardoso, *Int. J. Theor. Phys.* **12**, 1565 (1991).
[8] P.A.M. Dirac, *Proc. Roy. Soc. London*, **A155**, 447 (1936).
[9] W.L. Bade, H. Jehle, *Rev. Mod. Phys.* **25**, 714 (1953).
[10] J.G. Cardoso, *Acta Phys. Pol.* **B24**, 1481 (1993).
[11] J.G. Cardoso, *Int. J. Mod. Phys.* **A8** (21), 3697 (1993).
[12] J.G. Cardoso, Theory of complexified Maxwell-Dirac fields, preprint, Quaid-i-Azam University, 1993.
[13] R. Geroch, A. Held, R. Penrose, *J. Math. Phys.* **14**, 874 (1973).
[14] J.G. Cardoso, *Int. J. Mod. Phys.* **A8** (14), 2437 (1993).
[15] F.G. Friedlander, *The Theory of Distributions*, CUP, Cambridge 1976.
[16] J.G. Cardoso, *J. Math. Phys.* **35**, 294 (1994).